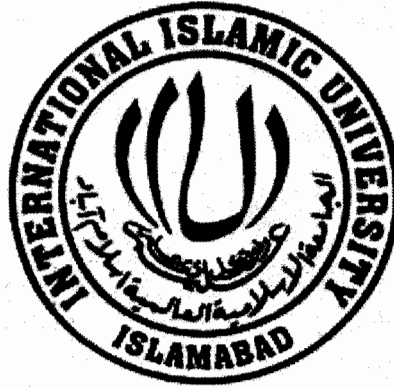


3-D Hemisphere Model with Antenna Array at BS for Wireless Radio Environment

TO 7483



MS (Electronics Engineering)

Thesis Submitted By:

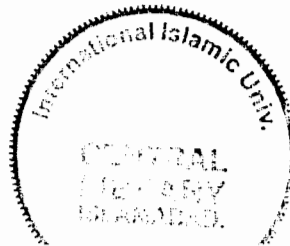
Mr. Rahat Ullah

Reg. No.98-FET/MSEE/F 07

Thesis submitted to the Faculty of Electronic Engineering in partial fulfillment of requirements
for the Degree MS (Electronic Engineering)
Spring-2010

Faculty of Engineering and Technology,

International Islamic University, Islamabad



Accession No. TH 7483

DATA ENTERED

CE
20/01/2012

MS
621-382
RAH


- 1- Wireless communication systems- Technological innovations
- 2- Antenna arrays
- 3- Antennas (electronics)

D-E
AC
3-3-11

FORWARDING SHEET

The thesis entitled "3D Hemisphere Model with Antenna Array at the BS for Wireless Radio Environment" submitted by Mr. Rahat Ullah Registration No. 98/FET/MSEE/f-07, in partial fulfillment of Master degree in Electronic Engineering, has been completed under my guidance and supervision. I am satisfied with the quality of student's research work and allow him to submit this thesis for further process of as per IIU rules & regulations.

Date: 02-03-10

Supervisor Signature: 

Name : Dr. Ataul Aziz Ikram

Thesis Declaration



Certified that the work contained in this thesis entitled

3-D Hemisphere Model with Antenna Array at BS for Wireless Radio Environment

is totally my own work and no portion of the work referred in this thesis has been submitted in support of an application for another degree or qualification of this or any other institute of learning.

Rahat Ullah

89/FET/MSEE/F-07

Dedicated to

My Beloved Parents

ACKNOWLEDGEMENTS

In the name of Allah, the Most Gracious and the Most Merciful

All praise and glory to Almighty Allah (Subhanahu Wa Ta'ala) who gave me the courage and patience to carry out this work. Peace and blessings of Allah be upon His last Prophet Muhammad (Sallulaho-Alaihe-Wassalam).

First and foremost gratitude is due to the esteemed university, the International Islamic University Islamabad for my admittance, and to its learned faculty members for imparting quality learning and knowledge with their valuable support and able guidance that has led my way through this point of undertaking my research work.

I am sincerely indebted to my thesis supervisor, **Dr. Ata Ul Aziz Ikran**, for his continuous guidance, valuable advice, immense effort, and thoughtful discussions throughout my research. It was surely an honor and an exceptional learning to work with him.

I wish to thank my colleague Syed Junaid Nawaz for introducing me this topic and for all his encouragement and support. Especially, I would like to thank my friend and colleague Engr. Hanif Ullah for his constant moral support throughout my thesis work. Sincere friendship is the spice of life. I owe thanks to my house mates and my friends for their motivation and pivotal support.

I would like to thank my Family, specially my parents for all their love, understanding and support. Their prayers and encouragement always help me to take the right steps in life. Special thanks to my uncle Aziz ur Rahim, for all his motivation and support throughout my academic carrier. Without my family, my success would not be possible.

Abstract

Development of realistic channel model that efficiently and accurately describes spatial characteristics of the wireless channel is one of main research area in the field of communication engineering. Spatial characteristics of the wireless radio channel include Angle of Arrival (AoA) and Time of Arrival (ToA) statistics. To utilize the spatial domain parameters effectively it is vital to have reliable understanding of radio propagation path between base station (BS) and mobile station (MS). Moreover, in the past years, it has been shown in theory and practice that with the use of smart antenna technology, performance of the wireless communication systems can be improved. The use of smart antenna can improve the quality of service and enhance system capacity at affordable cost.

In this thesis, 3D Hemisphere Model with Antenna Array at the BS is proposed for a wireless radio environment, and AoA statistics at the MS are analyzed. Proposed model assumes uniformly distributed scatterers around the MS, located at the center of the hemisphere. Whereas the BS is located outside the hemisphere, and no scatterers are assumed around it, because of its height. Close form expressions for the joint and marginal PDF of AoA at MS are derived mathematically, for both azimuth and elevation planes. Results are analyzed and it is shown that the proposed 3D model deduce all previous models that assume uniform distributions of scatterers around MS found in literature for macrocell environment. It is shown that when the beamwidth of the directional antenna at BS is set to its maximum, i.e. including complete scattering region of hemisphere, the spatial statistics are found to be the same as those found in 3D model by Janaswamy for omnidirectional antenna at the BS. In a similar way, all 2D models that assume uniform distributions of scatterers, whether directional or omni-directional found in literature for wireless radio environment can be deduced from proposed 3D model by substituting elevation angle equal to zero. The derived expression for the AoA statistics can be useful in the analysis of Doppler Shift in 3D radio environment, and the effect of directional antenna can be investigated. Also the proposed model can be further used to find the effect of directional antenna for which the beamwidth is controlled in elevation plane, on spatial characteristics of the wireless channel.

TABLE OF CONTENTS

THESIS DECLARATION	4
ACKNOWLEDGEMENTS	6
ABSTRACT	7
LIST OF FIGURES	10
LIST OF ACRONYMS	12
LIST OF NOTATIONS	14
CHAPTER NO. 1 INTRODUCTION	15
1.1 OVERVIEW	15
1.2 HISTORY OF CAPACITY ENHANCEMENT IN WIRELESS SYSTEMS.	16
1.3 MULTIPATH PROPAGATION	17
1.4 BACKGROUND	19
1.4.1 AOA ESTIMATION	19
1.4.2 SMART ANTENNA	20
1.4.3 SPATIAL CHANNEL MODELING	20
1.5 PROBLEM FORMULATION	20
1.6 METHODOLOGY	21
1.7 ORGANIZATION OF THE THESIS	21
CHAPTER 2 LITERATURE REVIEW:	22
CHAPTER 3 3D HEMISPHERE MODEL WITH ANTENNA ARRAY AT BS.	30
3.1 INTRODUCTION	30
3.2 PROPOSED 3D HEMISPHERE MODEL WITH ANTENNA ARRAY AT BS	32
3.3 DERIVATION OF THE SCATTERERS VOLUME AND LIMITS	34
3.3 DERIVATION OF JOINT AOA STATISTICS	37
3.4 DERIVATION OF MARGINAL AOA STATISTICS	39

CHAPTER 4 RESULTS AND DISCUSSIONS	41
4.1 THRESHOLD ELEVATION ANGLE Θ_{THRESH} AS FUNCTION OF AZIMUTH ANGLE:	41
4.2 THRESHOLD AZIMUTH ANGLE "Φ_{THRESH}" AS FUNCTION OF ELEVATION ANGLE:	42
4.3 PLOT OF LENGTH L "DISTANCE BETWEEN THE MS AND SCATTERERS"	42
4.4 ANALYTICAL RESULTS OF PDF OF AOA AT MS.	45
4.5 COMPARISON WITH SOME NOTABLE MODELS FOUND IN LITERATURE	48
4.6 EFFECT OF ADAPTIVE ANTENNA ARRAY ON AOA STATISTICS	51
CHAPTER 5 CONCLUSIONS AND FUTURE RESEARCH PLANS	53
5.1 SUMMARY OF THE THESIS	53
5.2 FUTURE RESEARCH PLANS	54
5.2.1 RESEARCH PLAN 1	54
5.2.2 RESEARCH PLAN 2	54
REFERENCES:	55

List of Figures

Figure1. 1: Different Causes Multipath in Wireless Communication	17
Figure1. 2: A Typical Wireless Radio Environment	18
Figure1. 3: Effect of Fading on signal strength	18
Figure1. 4: Smart Antenna Technology.....	19
Figure2. 1: Single Bounce Geometrical Model	22
Figure2. 2: 2D circular model	23
Figure2. 3: 2D elliptical model.....	23
Figure2. 4: Petrus proposed model [6]	24
Figure2. 5: Ertel's Model [8]	24
Figure2. 6: Richard B. Ertel Circular Model [7] for AoA PDF	25
Figure2. 7: Richard B. Ertel Elliptical Model [7] for AoA PDF	25
Figure2. 8: Single Bounce circular model proposed in [9]	26
Figure2. 9: Single Bounce elliptical model proposed in [9].....	26
Figure2. 10: Hollow Disc Scattering around MS [13]	27
Figure2. 11: A typical 3D model [11]	28
Figure2. 12: Geometry of the Model propoed in [12]	29
Figure3. 1: Proposed 3D Hemisphere Model	31
Figure3. 2: Azimuth and Elevation Plane view of the proposed model.....	32

Figure3. 3: Volume of the scatterers (Illuminated and eliminated)	33
Figure3. 4: Geometry of the truncated volume	33
Figure3. 5: Azimuth Angles ϕ_{thresh1} and ϕ_{thresh2} Geometry.....	35
Figure3. 6: Threshold Elevation Angle θ_{thresh}	36
Figure4. 1: Threshold Angle θ_{thresh} in Azimuth Plane.....	41
Figure4. 2: Threshold Angle Φ_{thresh} in elevation plane	42
Figure4. 3: Length L as a Joint Function of Azimuth and Elevation Plane.....	43
Figure4. 4: Distance L in Elevation Plane.	44
Figure4. 5: Distance L in Azimuth Pane for Different Elevation Angles	45
Figure4. 6: Joint PDF of AoA at MS for proposed 3D model	46
Figure4. 7: Marginal PDF of AoA in Elevation Plane	47
Figure4. 8: Marginal PDF of AoA in Azimuth Plane.....	48
Figure4.9: Marginal PDF of AoA in Elevation Plane for Janaswamy Model [11].....	49
Figure4.10: Comparison with Janaswamy Model	50
Figure4.11: Comparison with 2D Petrus Model.....	51
Figure4.12: Effect of Adaptive Antenna Array of AoA Statistics.....	52

List of Acronyms

1 G	First Generation of Land Mobile Systems
2 G	Second Generation of Land Mobile Systems
3 G	Third Generation of Land Mobile Systems
2D	Two Dimensional (Scattering Model)
3D	Three Dimensional (Scattering Model)
AoA	Angle of Arrival
AMPS	Advanced Mobile Phone Services
BLAST	Bell Laboratories Layered Space Time
BS	Base Station
CDF	Commutative Density Function
CDMA	Code Division Multiple access
DoA	Direction of Arrival
DoD	Direction of Departure
GBSBM	Geometrical-based Single Bounce Macrocell Model
GBSBCM	Geometrical Based Single Bounce Circular Model
GBSBEM	Geometrical Based Single Bounce Elliptical Model
GSM	Global System for Mobile Communication
ISI	Inter Symbol Interference
LCR	Level Crossing Rate
LOS	Line of Sight
MS	Mobile Station
MIMO	Multiple Input Multiple Output
NMT	Nordic Mobile Telephony
OFDM	Orthogonal Frequency Division Multiple Access
PAS	Power Azimuth Spectrum
PDS	Power Delay Spectrum

PDF	Probability Density Function
RMS	Root Mean Square
TDMA	Time Division Multiple Access
ToA	Time of Arrival
UMTS	Universal Mobile Telecommunication Systems
V-BLAST	Vertical Bell Laboratories Layered Space Time
WCDMA	Wideband Code Division Multiple Access

List of Notations

α	Beamwidth of directional antenna used at BS in 3D Hemisphere model
α_{max}	Maximum Beamwidth of the directional Antenna
$\Phi_{thresh1}$ & $\Phi_{thresh2}$	The angles in azimuth plane as a function of beamwidth of directional antenna used at BS
θ_{ms}	The elevation angle at MS in 3D scattering model
Φ_{ms}	The azimuth angle at MS in 3D scattering model
β_{thresh}	The threshold angle in elevation plane in proposed 3D model
D	Distance between BS and MS
H_t	Height of the BS in 3D scattering model
L	Distance Between the MS and the Scatterer
$P(L, \Phi_{ms}, \theta_{ms})$	Joint function as function of L , Φ_{ms} and θ_{ms}
$g(x,y,z)$	Scatterers density function
$J(x,y,z)$	Jacobian Transformation
$P(\Phi_{ms}, \theta_{ms})$	Joint PDF of the AoA in Azimuth and Elevation plane at MS
$P(\Phi_{ms})$	Marginal PDF of AoA in Azimuth Plane at MS
$P(\theta_{ms})$	Marginal PDF of AoA in Elevation Plane at MS
R	Radius of the Hemisphere
V_{sphere}	Volume of the Sphere

Introduction

1.1 Overview

During the past few decades the world has observed tremendous development in the telecommunication industry due to ever increasing demands for capacity enhancement, higher data rates and quality of service. Capacity enhancement is one of the bigger research issues in cellular and mobile communication [18,20]. In the past years, resources of power and frequency have been used professionally with spectral signal processing techniques to accomplish the goal of capacity enhancement and quality of service. However, less concentration has been given to the spatial aspects of the wireless radio channel [1]. Development of realistic channel model that efficiently and accurately describes spatial characteristics of the wireless channel is one of main research area in the field of communication engineering [12]. Spatial characteristics of the wireless radio channel include Angle of Arrival (AoA) and Time of Arrival (ToA) statistics. To utilize the spatial domain parameters effectively it is vital to have reliable understanding of radio propagation path between base station (BS) and mobile station (MS) that leads to the design of efficient signal processing techniques [2]. Moreover, in the past years, it has been shown in theory and practice that with the use of smart antenna technology, performance of the wireless communication systems can be improved. The use of smart antenna can improve the quality of service and enhance system capacity at affordable cost [3].

1.2 History of Capacity enhancement in wireless systems.

In wireless communication systems the increasing demand of capacity has always been an essential objective [18]. The concept of cellular concept was introduced at Bell Labs in 1980. The idea of frequency reuse was introduced by AT&T in 1968- 70 to attain high capacity in analog cellular telephone system called the Advanced Mobile Phone Services (AMPS). AMPS was the first U.S cellular telephone system that uses frequency division multiple access (FDMA) technique to enhance capacity. First cellular system was Nordic Mobile Telephony (NMT) in Europe. It was developed in Sweden in 1981 but mainly for Sweden, Denmark, Finland & Norway. U.K developed an indigenous standard called Total Access Communication System (TACS) in 1985. The analog cellular mobile systems belonging to that era of time are known as the First Generation (1G) wireless technologies. Since then wireless systems has seen rapid progress using digital communication technology and transformed into a new era of the Second Generation (2G) wireless systems. The 2G wireless technologies comprise Global System for Mobile Communication (GSM), IS – 136 and IS – 95. GSM was initially called Groupe Spatial Mobile and was develop in the early 1980s. The GSM launched in 1990 using time division multiple access (TDMA) to accommodate a large number of subscribers. On the other hand IS – 136 and IS– 95 uses Code Division Multiple Access (CDMA). Application such as multimedia service and mobile internet require high capacity and data rates. These demands have led to the development of the Third Generation (3G) wireless technologies. 3G systems are more sophisticated in terms of capacity, data rates, security and services. The most important technology in 3G is Universal Mobile telecommunication Systems (UMTS). Other standards include Wideband CDMA (WCDMA) and CDMA 2000.

To improve reliability at the transmitter and receiver sides multiple antennas are used for diversity. Through the use of multiple antennas and intelligent signal processing e.g. the knowledge of angle of arrival, it is possible for smart antennas to adjust its beam pattern to a particular area and hence provide optimal gain and minimize interference [3]. The use of MIMO (multiple-input multiple-output) technology, has rapidly gained popularity over the past decade due to its influential performance enhancing potentials. The use of adaptive antenna array in the next generation mobile communication has raised significant interest during last year's [1]. Their capability of capacity enhancement is considerable but realistic channel modeling that describe

both temporal and spatial characteristics, is one of the primary requirement for performance evaluation of the wireless systems [12]. With the use of smart antennas multiple user can share the same air interface and hence improve capacity of the system [4]

1.3 Multipath Propagation

In wireless systems received signal strength and phase are change rapidly because of the varying nature of the wireless radio environment. Moreover the transmitted signal gets reflected by different objects (buildings, different means of transportation on the ground, etc) as shown in Figure 1.1 leading to different paths to the receiver with different individual path parameters. The presence of scatterers in radio environment causes fading. Fading is the rapid fluctuation in signal amplitude of a radio signal over short instant of time or traveled distance [5].

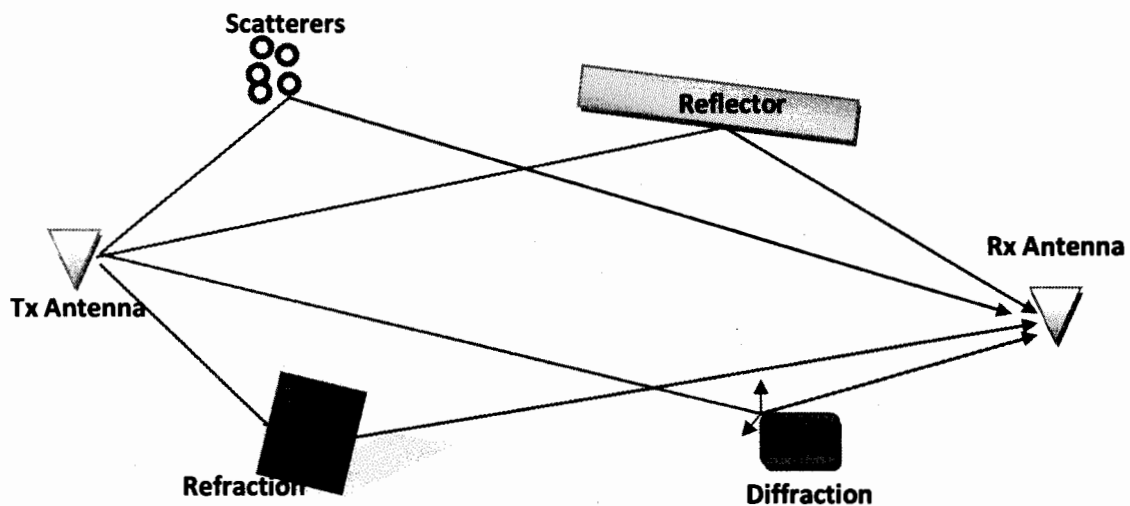


Figure1. 1: Different Causes Multipath in Wireless Communication

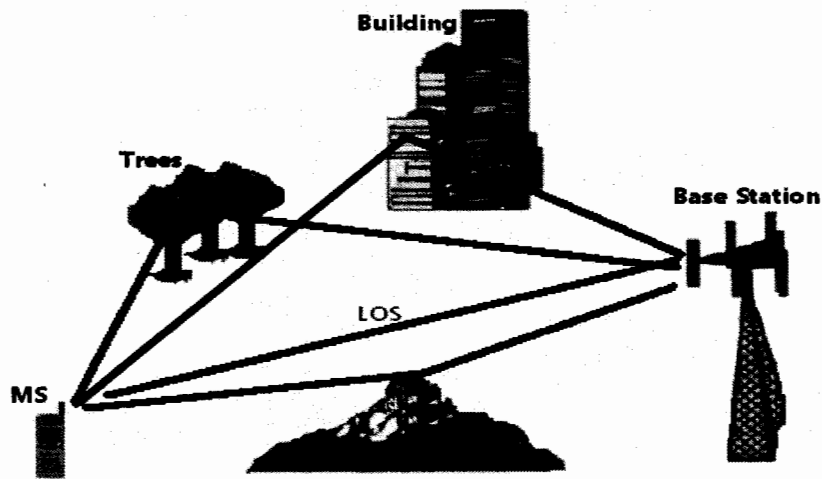


Figure1. 2: A Typical Wireless Radio Environment

The effect of fading on signal strength is shown in Figure 1.3. When two or more versions of the transmitted signals are received with a slightly different time at the receiver, interference is experienced [5]. Multipath signal combines at the receiving antenna to give a resultant signal which can vary in delay, amplitude and phase.

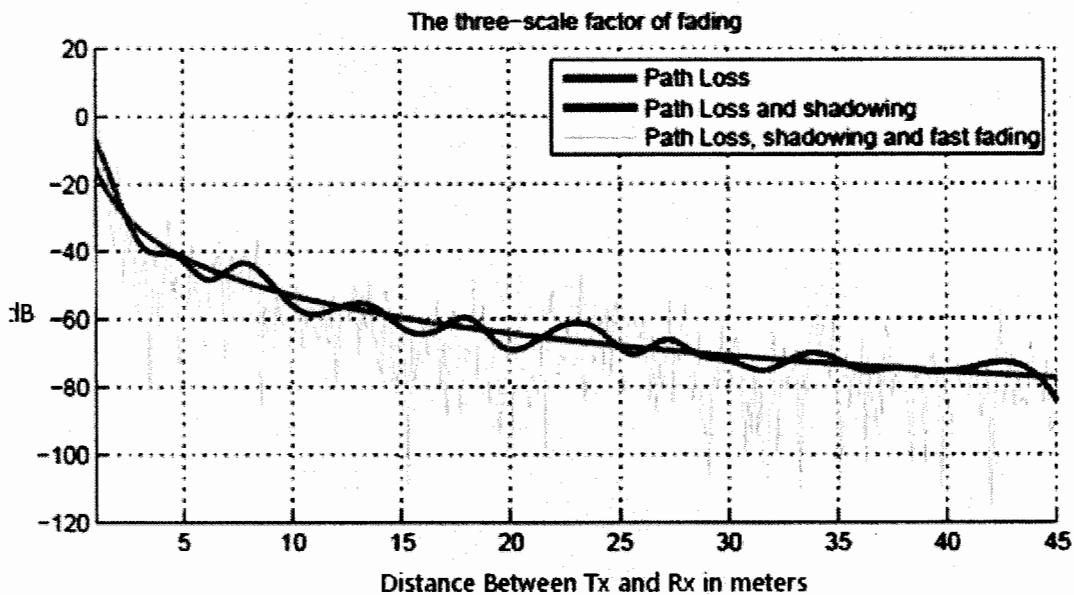


Figure1. 3: Effect of Fading on signal strength

A good understanding of the physical channel is necessary in order to observe the spatial characteristics of the multipath components. To accomplish this objective different 2D and 3D Geometric models have been presented in literature for mobile radio environment. In wireless

radio propagation, the multipath components coming from scatterers that are closer to mobile station are more dominant than those which are at a larger distance. Furthermore, in almost all 2D and 3D models proposed in the literature, single bounce scattering is assumed because multiple bounce diminish the signal power rapidly.

1.4 Background

1.4.1 AoA estimation

For macrocell cell radio environment shown in Figure1.2 it is obvious that even for a single source there are many possible multipath and angles of arrival. Therefore it is necessary for the receiving array to be able to have knowledge of the AoA in order to determine the angular location of the emitters present. Such information is useful to reduce signal of greater fidelity and for interference suppression [3]. AoA estimation is also known as spectral estimation or direction of arrival estimation [4].

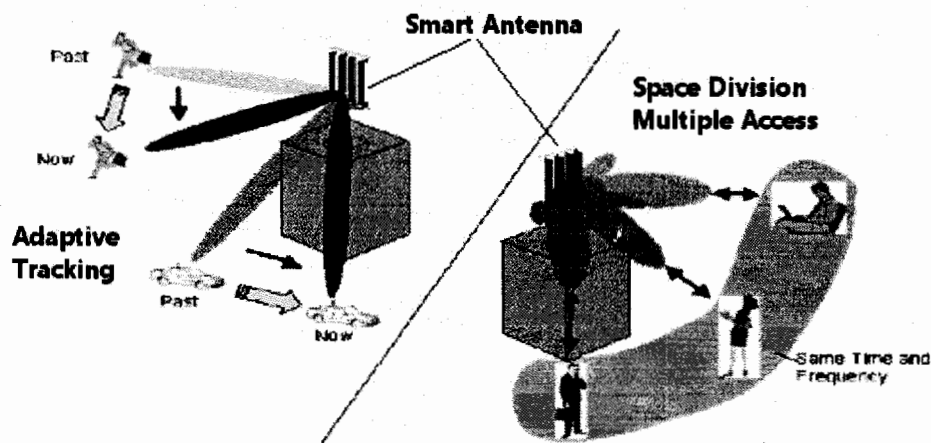


Figure1. 4: Smart Antenna Technology

Spectral estimation is the capability to select a range of frequency components from a set of signal. There are different algorithms proposed in literature for AoA estimation. If a transmitter is employed with antenna array and prior knowledge of AoA, it can adaptively adjust its parameters to radiate its beam pattern in a particular direction as shown in Figure1.4. Hence interference can be reduced and quality of service will improve.

1.4.2 Smart Antenna

Smart antenna refer to any antenna array with digital signal processing capability that can adaptively adjust its beam pattern in particular area of interest and minimize interference[4]. The use of smart antennas can improve the quality of service and enhance system capacity at affordable cost [3]. Smart antennas generally include both switched beam and beamformed adaptive systems. Switched beam systems have several available fixed beam patterns. The access of any beam among the fixed pattern at any time instant is based on the system requirements. Beamformed adaptive systems allow the antenna to adjust the beam to any direction of interest while at the same time nulling interfering signals. Figure 1.4 shows how smart antenna technology is used in beam tracking and adaptive beam formation for a particular area of interest.

1.4.3 Spatial Channel Modeling

Development of a realistic channel model, that can efficiently describe the spatial and temporal characteristics, is one of the major objectives of communication engineering [12]. In almost all geometrical models proposed in literature, it is assumed that one scatter between the transmitter and receiver. The spatial characteristics for wireless radio channel have been investigated extensively in two dimensional (2D) models. In a typical macrocell environment, the distance between the MS and BS is large and hence the effect of elevation angle is minimal. So in 2D models the channel spatial characteristics have been observed in azimuth plane only. BS antenna is assumed to be surrounded by a scattering free region because of its high altitude. Whereas, the MS is assumed to be surrounded by scattering objects either in circular or elliptical geometry.

1.5 Problem Formulation

In order to meet the increasing demand with respect to capacity, the resources of frequency and power have been used extensively. The spectral signal processing techniques alone cannot meet the increasing demand of capacity [1]. The spatial characteristics of the mobile channel are proven to be helpful in order to furnish and accommodate such needs. Therefore, an understanding of the physical channel is required to exploit these spatial characteristics [2]. It has been observed that PDF of AoA at MS is found rigorously in 3D scattering model. Some authors use the directional antennas at BS in 2D scattering model. However to the best of the author's

knowledge, adaptive antenna array has never been used at BS for a 3D hemisphere model. Moreover, in 3D scattering model the PDF of AoA in closed form simultaneously in azimuth and elevation plane has never been observed using directional antenna. The problem can be formulated to investigate the spatial characteristics in closed form simultaneously in azimuth and elevation plane using directional antenna at BS in 3D scattering model.

1.6 Methodology

To derive the expression for PDF of AoA for wireless radio environment while directional antennas used at BS the result of [6] for beamwidth calculation are used in modified form. The 2D geometrical model [7] is also used for modeling and characterization of mobile radio channels. 3D semi-spheroid model proposed by Janaswamy [11] is modified to 3D hemisphere with antenna array at BS is used for the derivation of the PDF of AoA in close form simultaneously in azimuth and elevation plane.

1.7 Organization of the Thesis

The rest of the thesis is organized as follows: Literature Study is presented in Chapter No.2. In Chapter 3 the proposed 3D Hemisphere Model with Antenna Array at BS is presented with mathematical derivations of the PDF of AoA. Results and discussions are presented in Chapter No.4. Finally, conclusions and future research plans are given at Chapter No.5

Literature Review:

The performance of wireless system has improved in recent years as the demand for capacity has increased. One area of interest within wireless communication is the development of realistic channel models that efficiently describe the characteristics of the channel. Channel models that correctly provide the spatial and temporal characteristics are mostly used for performance evolution of wireless systems [12]. A rich literature exists on rigorous mathematical derivations of spatial and temporal characteristics. The angle of arrival statistics have been widely studied in azimuth plane for mobile radio environment mostly in 2D geometrical models. To minimize the effect of interference because of the multipath components, adaptive antennas with phase shift techniques are proposed in literature. The use of smart antenna can improve quality of service and enhance system capacity at affordable cost [3]. However to achieve the objective of capacity enhancement and quality of service fixed beam directional antennas are also a good option.

In most of the models proposed in literature a single bounce scattering is assumed around the MS with different distribution. In Single Bounce Models, single scatterer is assumed in the propagation path between the MS and BS as shown in Figure 2.1. The signal power decreases rapidly with multiple bounces, and that is the reason why most of the model proposed in literature assumes single bounce of the signals. The study of spatial characteristics of the wireless channel are available in 2D [3,4,7,8,9,14&21] as well as for 3D [11,12,13,14,15] geometrical models.

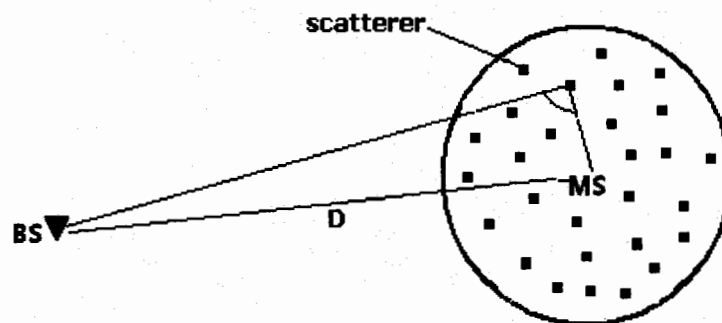


Figure2. 1: Single Bounce Geometrical Model

In 2D geometrical model MS is assumed to be located at the center of the scattering region which may be a circle or an ellipse in azimuth plane, while the BS is usually located above the ground. Circular and elliptical channel models are shown in Figure 3.2 and 3.3 respectively. In models proposed in literature for macrocell environment, the BS antenna is assumed to be surrounded by scattering free region while MS is assumed to be surrounded by scattering objects [18]. In microcell environment the scatterers are assumed in the region around the BS because the antenna height is low.

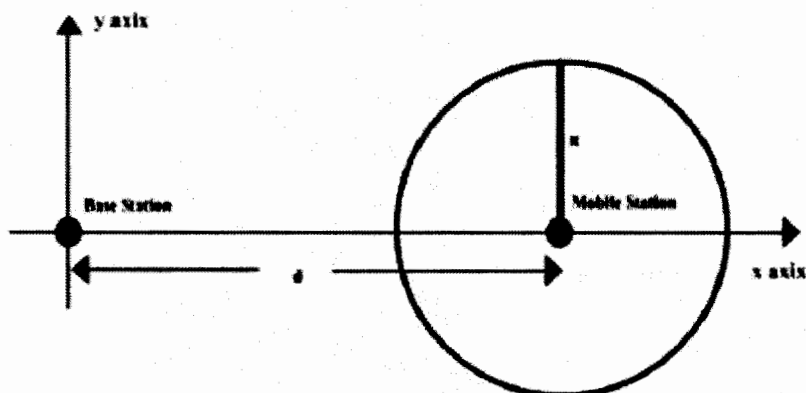


Figure2. 2: 2D circular model

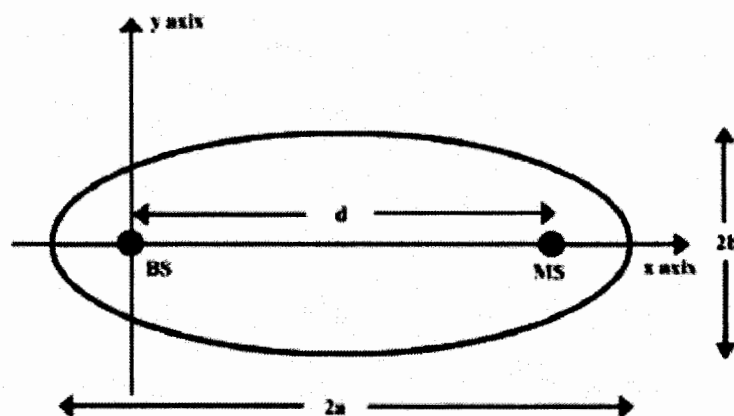


Figure2. 3: 2D elliptical model

In [6] Paul Petrus, proposed a geometrically based single bounce macrocell (GBSBM) channel model using directional antenna at BS. His proposed model is shown in Figure 2.4. Petrus model is based on the assumption that scatterers are uniformly distributed around the MS in a circular region with radius R . D is the distance between the MS and BS, and is greater than R for a macrocell radio environment. The BS is assumed to be elevated at some height and is assumed

to be in a scattering free region. The direction of arrival (DoA) as seen from BS can only be calculated in azimuth plane as the signals are assumed to be plane waves from different horizon.

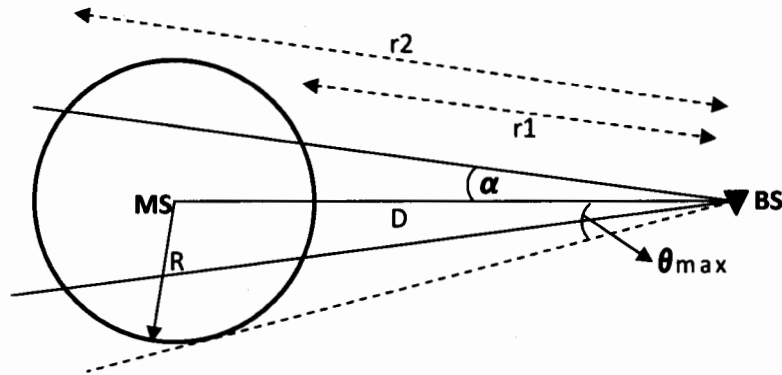


Figure2. 4: Petrus proposed model [6]

Power of the multipath components in addition to probability distribution function (PDF) of the angle of arrival (AoA) and time of arrival (ToA) of multipath components are presented in [6]. It has been concluded in [6] that the level crossing rate of the fading envelope decreases and the envelope correlation increases significantly if the base station antenna is employed with directional antenna.

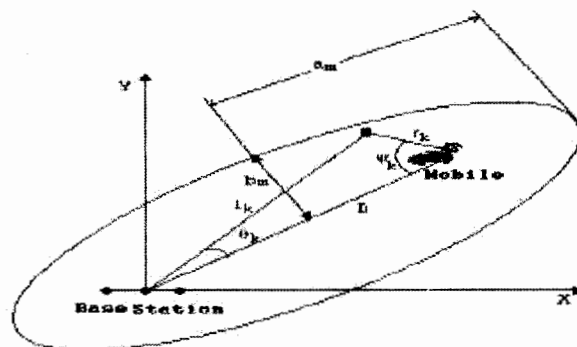


Figure2. 5: Ertel's Model [8]

Geometrical Based Single Bounce Elliptical Model (GBSBEM) is proposed by Leberti and Rappaport in [8] for a microcell radio environment. This model assumes the scatterers are distributed uniformly around the MS and BS that are placed at the foci of the ellipse. For a microcell radio environment the BS is assumed to be located at a low antenna height and hence

the scatterers are assumed around BS unlike macrocell environment where it is elevated at some height H_t . Figure 2.3 illustrate the geometry of the GBSBE Model.

In [7], Richard B. Ertel and Jeffrey H. Reed, proposed 2D single bounce elliptical and circular models and derived the PDF for AoA & ToA, where marginal PDF in angle and time is found from joint distribution of angle and time. In their study a common approach is used for both circular and elliptical model in the derivations of PDF for AoA & ToA, where in the Base station is assumed to have omni directional antenna.

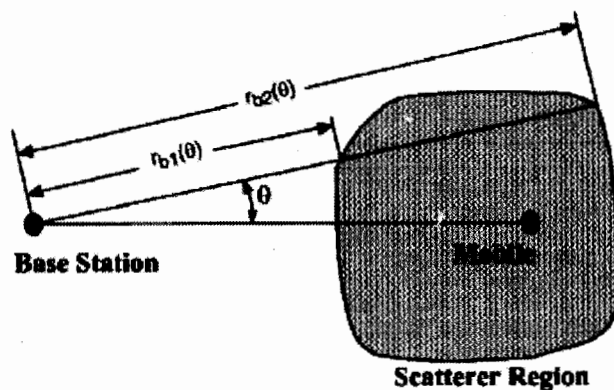


Figure2. 6: Richard B. Ertel Circular Model [7] for AoA PDF

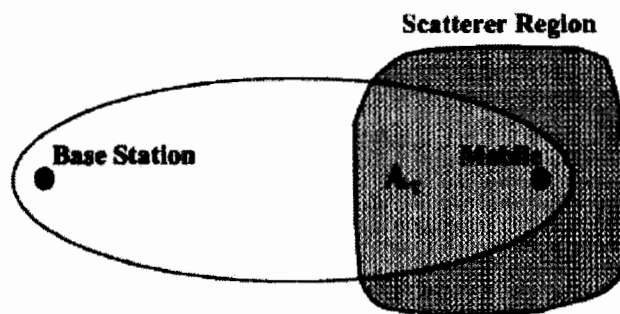


Figure2. 7: Richard B. Ertel Elliptical Model [7] for AoA PDF

In [9] a 2D circular and elliptical scattering model are proposed by Janaswamy, where the scatterers are assumed to have Gaussian density around the MS. PDF for AoA and ToA are calculated and the results are compared with experimental data measurements both for indoor

and outdoor environments. Close form expression is provide in terms of standard deviation for rms delay spread. This model is useful for both macrocell and picocell environments.

A similar kind of work is done in [10] by using Gaussian scatter density around MS where PDF of AoA is found at BS and MS respectively with directional antenna at the BS.

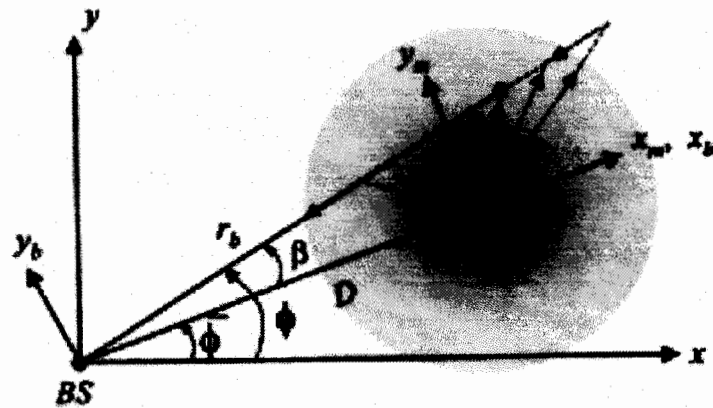


Figure2. 8: Single Bounce circular model proposed in [9]

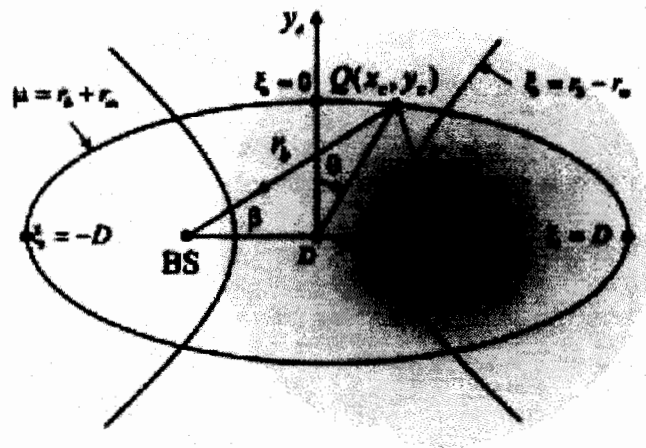


Figure2. 9: Single Bounce elliptical model proposed in [9]

In [13], Insaf Jafar proposed a 2D model in which the scatterers are assumed to be uniformly distributed around the mobile station in hollow disc and ellipse, and expression for joint and marginal PDF of the Time of Arrival (ToA) and azimuth angle of arrival (AoA) are derived. In the elliptical model, the mobile station and base station are assumed at foci points and the

scatterers are also assumed around the base station hence this is a more suitable approach for the microcell environment.

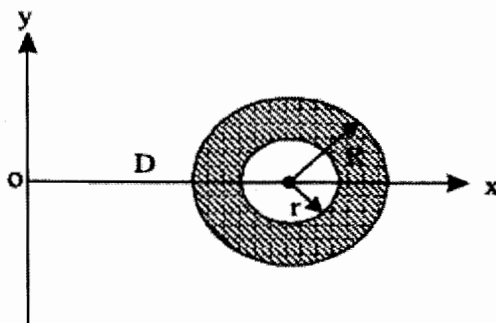


Figure2. 10: Hollow Disc Scattering around MS [13]

In [14] Sami A. Mostafa analyzed the effect of system geometry for GBSBCM and GBSBEM on the AoA statistics of the multipath components. It has been found that the effect of the maximum delay time and the distance between the MS and BS on the angle spread decreases in case of elliptical scattering density i.e for GBSEM. The angle spread changes rapidly in the case of smaller distance and a smaller delay of the multipath components with the same geometry. Similarly, for GBSBCM it is found that this model measurements are convincing when the radius of the circle is equal to the half of the distance between the MS and BS. In [21] Khoa N.le, new hyperbolic scatterer distribution has been proposed and the probability distribution function (PDF) for angle of arrival (AoA), time of arrival (ToA), power azimuth spectrum (PAS) and power delay spectrum (PDS) are derived. The results are compared with the experimental data along with the results of the previous models. In the comparison of results, it is shown that the assumption of hyperbolic distribution of scatterers around the MS is a closer match to experimental data [20].

In 2-D models, the characteristics of the wireless channel can't be perfectly analyzed because of the zero elevation planes [12]. The actual scenario can be visualized by 3D models. A typical 3D model allows us to determine the spatial characteristics both in azimuth and elevation plane. In 3D propagation models found in literature, the mobile radio environment has been visualized rigorously with low MS antenna. The BS antenna is assumed to be elevated at some height H_t above the ground with a scattering free region, whereas scatters are assumed to be distributed in a geometrical region around the MS. In almost all models proposed in literature the MS is assumed at the center of circular/spheroid geometry. It can be observed that 3D scattering model

has a close resemblance with realistic wireless mobile radio environment. A typical 3D model is shown in Figure 1.8.

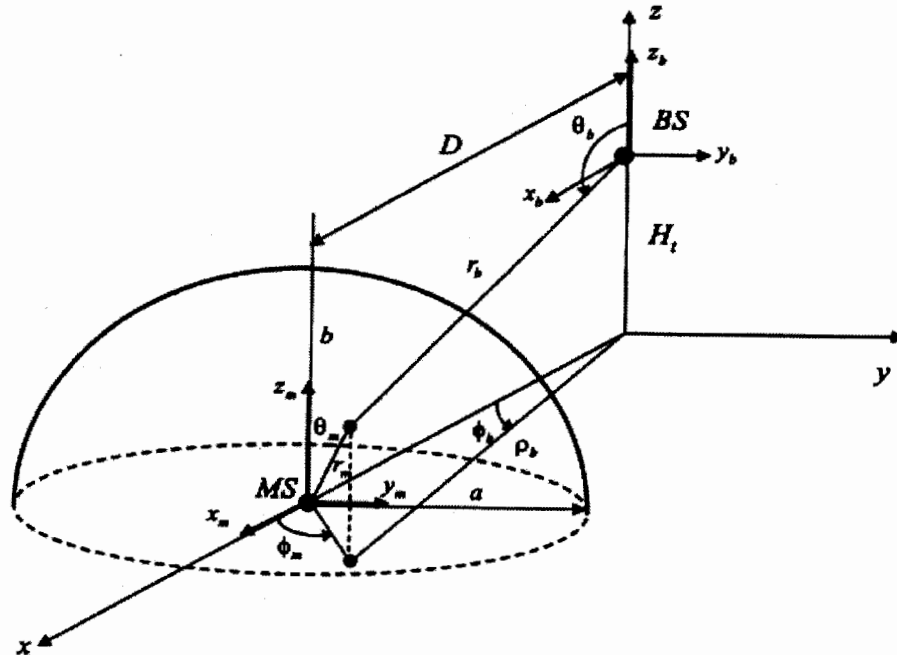


Figure2. 11: A typical 3D model [11]

A 3D geometrical scattering model is proposed in [11], by Janaswamy to describe the PDF of AoA of the multipath components as seen from mobile station and base station simultaneously in azimuth and elevation plane. The scatterers are assumed to be uniformly distributed around the mobile station in semispheroid geometry. The base station is elevated with omnidirectional antenna. The geometry of the Janaswamy model is shown in Figure 1.11.

Another 3D Geometric channel model is illustrated in [12], which is derived from a 2D Geometrical based single bounce macrocell (GBSBM) model, where the comparisons of 2D and 3D models published in literature have been shown in comparison with the experimental data. It is concluded that that the distance between the mobile station and base station, the height of the base station antennas and the geometry of the scatterers are more crucial for a 3D than 2D models[12].

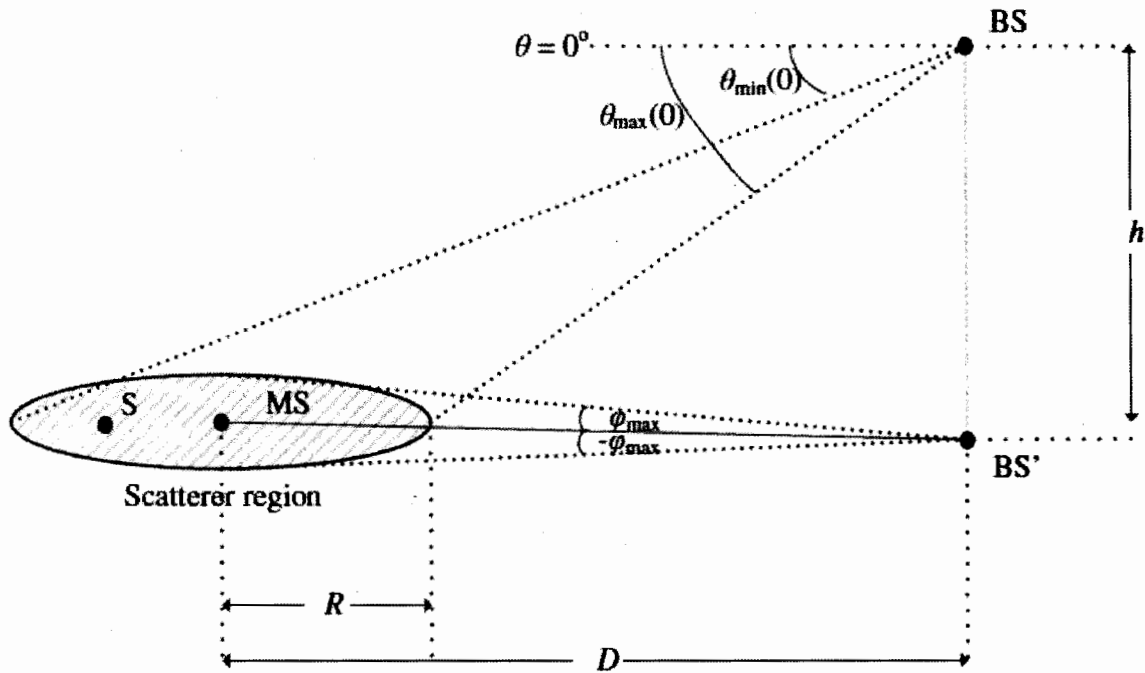


Figure 2.12: Geometry of the Model proposed in [12]

TH 7483

In [15] PDF of DoA and Time of Arrival (ToA) are derived analytically for uplink/downlink with the assumption that scatterers are uniformly distributed in a 3D hemispheroid around the MS located at the center of the geometry.

The power spectral density and PDF of AoA with non zero elevation plane is derived theoretically in [16] using 3D scattering model, where theoretical results are compared with the actual field measurement. A similar kind of model for 3D scattering environment is presented in [15 to 17] using ellipsoidal model for the derivation of direction of arrival (DoA) and direction of departure (DoD) in azimuth and elevation planes.

3D Hemisphere model with antenna array at BS.

3.1 Introduction

3D models are more realistic because they can be completely visualized and closely resemble the real life scenario of wireless radio channel. Thus 3D model offers more accurate spatial and temporal characteristics. A 3D semispheroid model is proposed in [11] by Janaswamy and AoA statistics of the multipath components as seen from BS and MS are derived. The PDF are derived for both azimuth and elevation planes. A similar 3D ellipsoidal model is proposed in [17], and PDF of the direction of arrival (DoA) and direction of departure (DoD) are derived simultaneously in azimuth and elevation planes. Another 3D Geometric channel model is presented in [12], which is the modified form of 2D Geometrical based single bounce macrocell (GBSBM) model proposed by Paul Petrus in [6]. In [12] close form expressions are given for the AoA statistics in azimuth and elevation plane and the results for 2D and 3D models are compared with the experimental data. In [15] PDF of DoA and Time of Arrival (ToA) are derived analytically for uplink/downlink with the assumption that scatterers are uniformly distributed in a 3D hemispheroid around the MS located at the center of the geometry. In [16] illustrating a 3D scattering model and the power spectral density and PDF of AoA with non zero elevation plane is derived theoretically, where theoretical results are compared with field measurement.

To achieve the objective of higher performance in terms of capacity in wireless systems we propose the use of directional antenna at BS in 3D scattering model for spatial characteristics of mobile channel. This is also shown in Figure3.1. The rest of the Chapter is organized as follows: Proposed 3D hemisphere model with directional antenna used at BS is described in section 3.2. Section 3.3 shows the joint and marginal PDFs of AoA at MS in azimuth and elevation planes. Similarly, the joint and marginal PDFs of AoA at BS in azimuth and elevation planes are given in section 3.4.

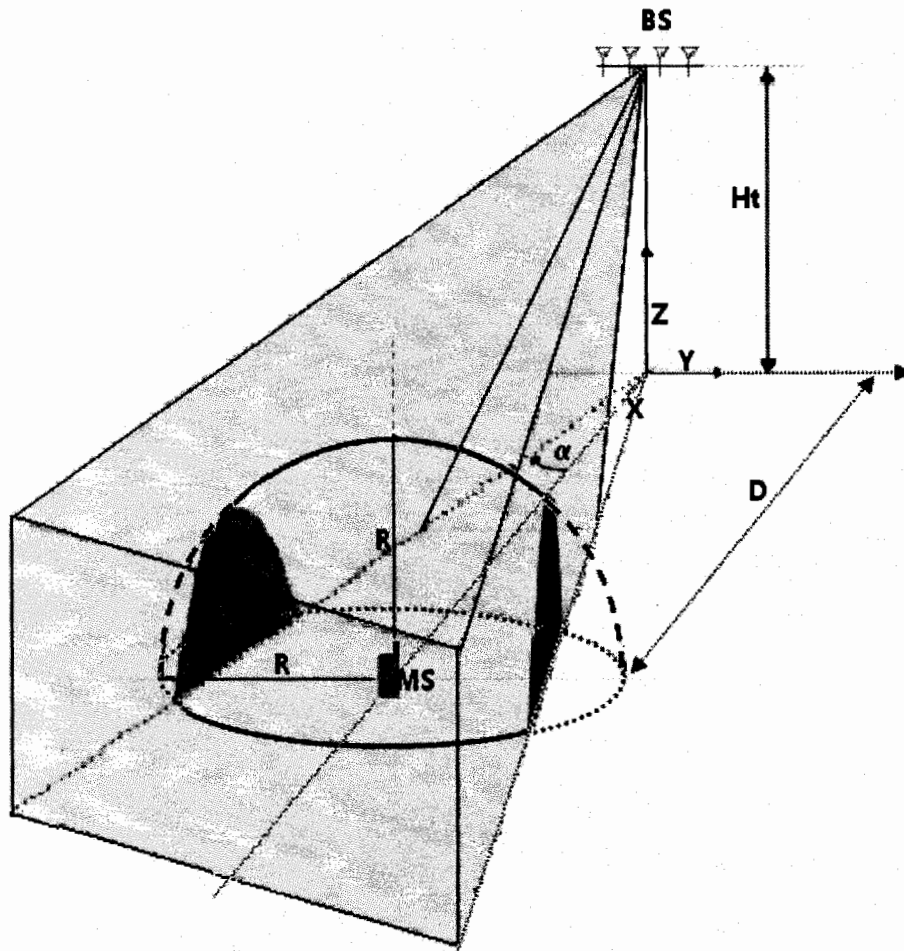


Figure3. 1: Proposed 3D Hemisphere Model

3.2 Proposed 3D hemisphere model with antenna array at BS

To achieve the goal of capacity enhancement and quality of service, a 3-D hemispheroid model is proposed in which adaptive directional antenna are positioned at BS and the beam-width is controlled in azimuth plane. The proposed 3-D propagation model used for the derivation of angle of arrival statistics with assumption that the scatterers are uniformly distributed around the MS. In this model mobile station MS is located at the center of the hemisphere as shown in Figure 3.1. The base station is employed with adaptive antenna array with beam width α at height H_t above the ground. The angles made by the direction of signal arrival in azimuth and elevation planes at MS are symbolized by Φ_{ms} and θ_{ms} and respectively as shown in Figure 3.2.

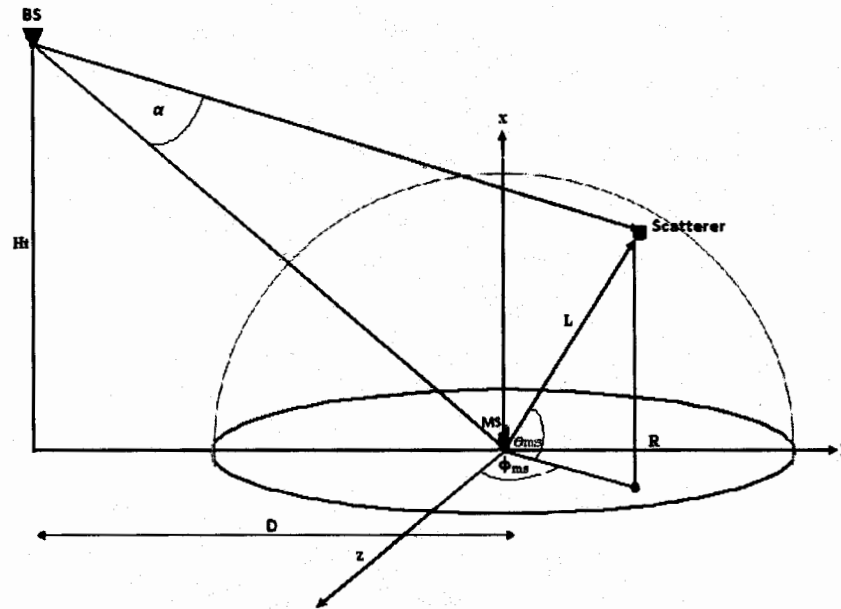


Figure3. 2: Azimuth and Elevation Plane view of the proposed model

When BS is equipped with adaptive antenna array the scatterers present in the complete hemisphere would not be illuminated, i.e. the hemisphere is partially illuminated. The volume of the region, whose scatterers are illuminated, is represented as V and the volume of the region, whose scatterers are not illuminated by the beamwidth of the directional antenna, is V_1 . The geometry of the illuminated and clipped region is shown in Figure 3.3.

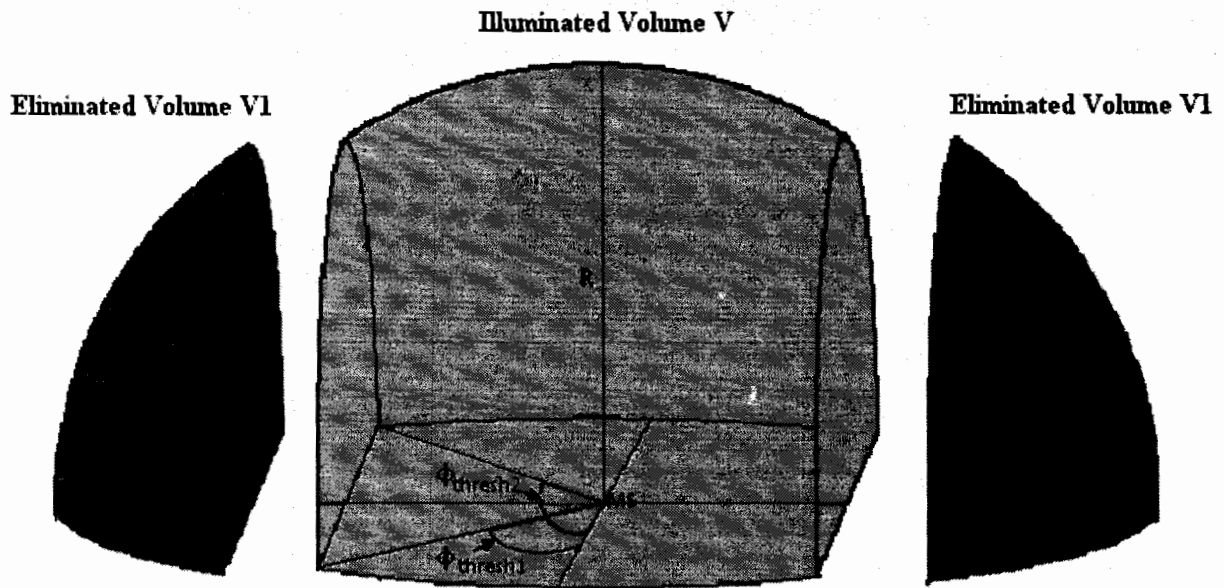


Figure3. 3: Volume of the scatterers (Illuminated and eliminated)

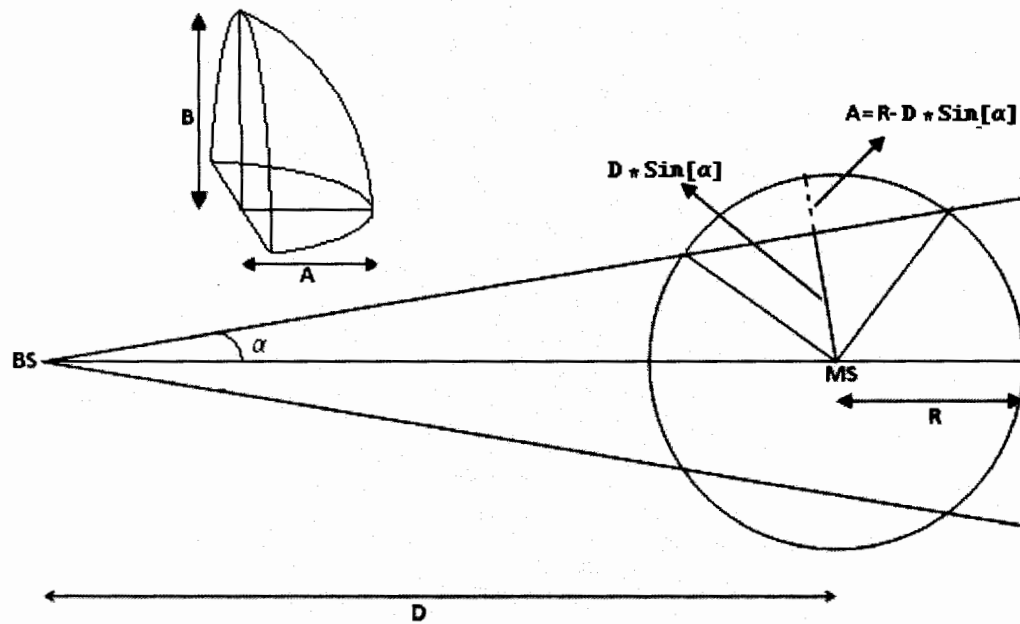


Figure3. 4: Geometry of the truncated volume

3.3 Derivation of the Scatterers Volume and limits

Volume of the sphere is given by following equation

$$V_{\text{sphere}} = \frac{4}{3} \pi R^3 \quad (3.1)$$

It can be seen from the geometry that the length A and B can be derived as

$$A = R - D \sin[\alpha] \quad ; \quad B = \sqrt{R^2 - D^2 \sin^2[\alpha]} \quad (3.2)$$

The volume of the truncated region is given by

$$V_1 = \frac{2}{3} \pi (R - D \sin[\alpha])^2 (R + D \sin[\alpha]) \quad (3.3)$$

Volume of the scatterers around the MS will be

$$V = \left(\frac{V_{\text{sphere}}}{2} \right) - 2 (V_1) \quad (3.4)$$

Hence substituting the values from equation 3.1 and 3.3 in equation 3.4 give the following relation

$$V = \frac{2}{3} \pi (R^3 - 2 (R - D \sin[\alpha])^2 (R + D \sin[\alpha])) \quad (3.5)$$

Equation 3.5 give the volume of the region around the MS where the scatterers are distributed uniformly shown in Figure 3.3. When the beam width of the directional antenna is set equal or greater than α_{max} all the scatterers inside hemisphere get illuminated. If we substitute $\alpha = \alpha_{\text{max}}$ in (3.5) the volume deduces to $V = 2/3 \pi R^3$ which is the volume of the hemisphere. The maximum beamwidth is given by

$$\alpha_{\text{max}} = \sin^{-1} \left(\frac{R}{D} \right) \quad (3.6)$$

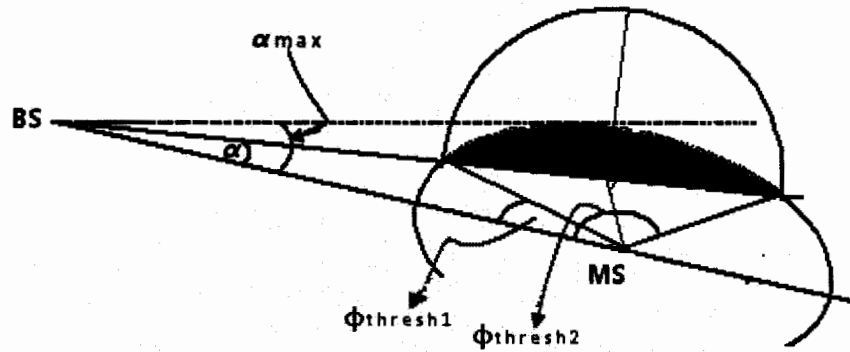


Figure3. 5: Azimuth Angles ϕ_{thresh1} and ϕ_{thresh2} Geometry

Threshold angles Φ_{thresh1} and Φ_{thresh2} cut these two different portions in azimuth plane of illuminated region as shown in Figure 3.6. These angles can be found as a function of elevation angle and beamwidth. The two angles are helpful in understanding the azimuth geometry of the 3D hemisphere model.

$$\phi_{\text{thresh1}} = \begin{cases} \cos^{-1} \left[\frac{\sec[\theta_{\text{ms}}] \left(D \sin[\alpha]^2 + \cos[\alpha] \sqrt{R^2 \cos[\theta_{\text{ms}}]^2 - D^2 \sin[\alpha]^2} \right)}{R} \right] ; & 0 \leq \theta_{\text{ms}} < \cos^{-1} [D \sin[\alpha] / R] \\ \pi / 2 - \alpha & ; \cos^{-1} [D \sin[\alpha] / R] \leq \theta_{\text{ms}} < \pi / 2 \end{cases} \quad (3.7)$$

$$\phi_{\text{thresh2}} = \begin{cases} \cos^{-1} \left[\frac{\sec[\theta_{\text{ms}}] \left(D \sin[\alpha]^2 - \cos[\alpha] \sqrt{R^2 \cos[\theta_{\text{ms}}]^2 - D^2 \sin[\alpha]^2} \right)}{R} \right] ; & 0 \leq \theta_{\text{ms}} < \cos^{-1} [D \sin[\alpha] / R] \\ \pi / 2 - \alpha & ; \cos^{-1} [D \sin[\alpha] / R] \leq \theta_{\text{ms}} < \pi / 2 \end{cases} \quad (3.8)$$

Similarly we can find the threshold elevation angle θ_{thresh} as a function of azimuth angle and the beamwidth α . The geometry of the threshold elevation angle is illustrated in Figure 3.7

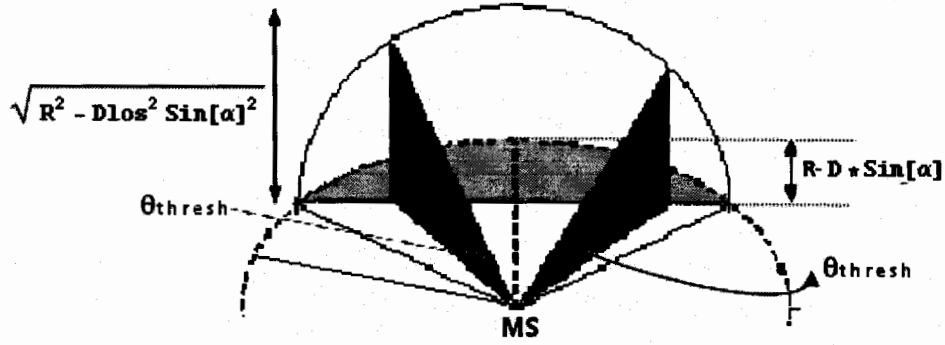


Figure3. 6: Threshold Elevation Angle θ_{thresh}

Close form equation for the threshold elevation angle θ_{thresh} is presented below.

$$\theta_{thresh} = \begin{cases} 0 & ; -\phi_1 \leq \phi_{ms} \leq \phi_1 \text{ or } \phi_2 \leq \phi_{ms} \leq -\phi_2 \\ \text{ArcCot} \left[\frac{D \text{Csc}[\alpha + \phi_{ms}] \text{Sin}[\alpha]}{\sqrt{L^2 - D^2 \text{Csc}[\alpha + \phi_{ms}]^2 \text{Sin}[\alpha]^2}} \right] & \text{otherwise} \end{cases} \quad (3.9)$$

The limits in the azimuth and elevation angles can be grouped as limit1 and limit2 for both regions which are given as follow

$$\text{Limit 1} = \begin{cases} \theta_{thresh} \leq \theta_{ms} \leq \pi/2 \\ \& \\ 0 \leq \phi_{ms} \leq 2\pi \end{cases} \quad (3.10)$$

$$\text{Limit 2} = \begin{cases} 0 \leq \theta_{ms} \leq \theta_{thresh} \\ \& \\ |\phi_1| \leq \phi_{ms} \leq |\phi_2| \end{cases} \quad (3.11)$$

It is very clear from Figure3.4 that if the elevation angle θ_{ms} is less than θ_{thresh} then the geometry of the model is solved by the proposed model using adaptive antenna array at the BS. This means that for this condition the beamwidth is less than α_{max} and the volume of region1 and region2 will be truncated and hence avoiding some of the scatterers of volume V1. Similarly

if the elevation angle θ_{ms} is greater than θ_{thresh} , then no volume is truncated and the scatterers of the complete hemisphere get illuminated. In this case the beamwidth of the directional antenna will be greater than or equal to α_{max} .

The distance between the MS and the scatterer, denoted by L , is calculated as

$$L = \begin{cases} R & ; \text{Limit 1} \\ D \cos[\phi_{ms}] \sin[\alpha] \sqrt{1 - \sin[\theta_{ms}]} & ; \text{Limit 2} \end{cases} \quad (3.12)$$

It is clear from equation 3.12 that if the beamwidth is greater than or equal to α_{max} then the distance between the MS and the scatterer is equal to R , which is the radius of the hemisphere. When the beamwidth is less than α_{max} then the distance between the scatterer and the MS can be found using expression for limit2

3.3 Derivation of Joint AoA Statistics

The joint expression as a function of L , azimuth angle Φ_{ms} and elevation angle θ_{ms} given by [7]

$$P(L, \phi_{ms}, \theta_{ms}) = \frac{g(x, y, z)}{|J(x, y, z)|} \begin{cases} x = L \cos\theta_{ms} \cos\phi_{ms} \\ y = L \cos\theta_{ms} \sin\phi_{ms} \\ z = L \sin\theta_{ms} \end{cases} \quad (3.13)$$

Where (x,y,z) and $(L, \Phi_{ms}, \theta_{ms})$ represent the position of the scatterer in the Cartesian and Spherical coordinates respectively.

The Jacobian Transformation $J(x,y,z)$ is given by

$$J(x, y, z) = \begin{vmatrix} \cos\theta_{ms} \cos\phi_{ms} & -L \cos\theta_{ms} \sin\phi_{ms} & -L \sin\theta_{ms} \cos\phi_{ms} \\ \cos\theta_{ms} \sin\phi_{ms} & L \cos\theta_{ms} \cos\phi_{ms} & -L \sin\theta_{ms} \sin\phi_{ms} \\ \sin\theta_{ms} & & \cos\theta_{ms} \end{vmatrix}^{-1}$$

$$J(x, y, z) = \frac{1}{L^2 \cos \theta_{ms}} \quad (3.14)$$

As the scatterers are assumed to be distributed uniformly around the MS in a hemisphere, the scatterer's density function can be written as

$$g(x, y, z) = \begin{cases} \frac{1}{V} & ; (x, y, z) \in \text{Illuminated Volume} \\ 0 & ; \text{Otherwise} \end{cases} \quad (3.15)$$

Using equation 3.13 and 3.14, the joint density function given by equation 3.12 can be rewritten as

$$P(L, \phi_{ms}, \theta_{ms}) = \frac{L^2 \cos[\theta_{ms}]}{V} \quad (3.16)$$

Putting the values of L and V from expression from 3.12 and 3.5 we have

In case of limit1 we have L=R so

$$P(L, \phi_{ms}, \theta_{ms}) = \frac{R^2 \cos[\theta_{ms}]}{2 \pi (R^3 - 2(R - D \sin[\alpha])^2 (R + D \sin[\alpha]))} \quad (3.17a)$$

In case of limit2, L is given by expression 3.12, and substituting the values in equation 3.15, we get

$$P(L, \phi, \theta) = \frac{3 (D \cos[\phi] \sin[\alpha] \sqrt{1 - \sin[\theta]})^2 \cos[\theta]}{2 (\pi (R^3 - 2(R - D \sin[\alpha])^2 (R + D \sin[\alpha])))}$$

OR

$$P(L, \phi, \theta) = \frac{D^2 \cos[\theta] \cos[\phi]^2 \sin[\alpha]^2 (1 - \sin[\theta])}{2 \pi (R^3 - 2(R - D \sin[\alpha])^2 (R + D \sin[\alpha]))} \quad (3.17b)$$

So the joint function

$$P(L, \phi_{ms}, \theta_{ms}) = \begin{cases} \frac{R^2 \cos[\theta_{ms}]}{2 \pi (R^3 - 2(R - D \sin[\alpha])^2 (R + D \sin[\alpha]))} & ; \text{Limit 1} \\ \frac{D^2 \cos[\theta_{ms}] \cos[\phi_{ms}]^2 \sin[\alpha]^2 (1 - \sin[\theta_{ms}])}{2 \pi (R^3 - 2(R - D \sin[\alpha])^2 (R + D \sin[\alpha]))} & ; \text{Limit 2} \end{cases} \quad (3.18)$$

The joint PDF of AoA in azimuth and elevation planes is found by integrating the above expression with respect to L or R with appropriate limits. The close form expression in simplified form after tedious calculations for joint PDF of AoA both in azimuth and elevation plane is given by

$$P(\phi_{ms}, \theta_{ms}) = \begin{cases} \frac{R^3 \cos[\theta_{ms}]}{2 \pi (R^3 - 2(R - D \sin[\alpha])^2 (R + D \sin[\alpha]))} & ; \text{Limit 1} \\ \frac{D^3 \cos[\theta_{ms}] \cos[\phi_{ms}]^3 \sin[\alpha]^3 (1 - \sin[\theta_{ms}])^{3/2}}{2 \pi (R^3 - 2(R - D \sin[\alpha])^2 (R + D \sin[\alpha]))} & ; \text{Limit 2} \end{cases} \quad (3.19)$$

3.4 Derivation of Marginal AoA Statistics

The marginal PDF of the AoA in azimuth plane found by integrating the above expression with respect to elevation angle θ with appropriate limits. The close form expression after tedious simplification for the marginal PDF of AoA seen from MS are presented in expression below

$$P(\phi_{ms}) = \begin{cases} \frac{R^3 \sin[\theta_{ms}]}{2 \pi (R^3 - 2 (R - D \sin[\alpha])^2 (R + D \sin[\alpha]))} & ; \text{Limit 1} \\ \frac{D^3 \cos[\phi_{ms}]^3 \sin[\alpha]^3 \left(\cos\left[\frac{\phi_{ms}}{2}\right] - \sin\left[\frac{\phi_{ms}}{2}\right] \right)^4 \sqrt{1 - \sin[\theta_{ms}]}}{5 \pi (R^3 - 2 (R - D \sin[\alpha])^2 (R + D \sin[\alpha]))} & ; \text{Limit 2} \end{cases} \quad (3.20)$$

In the above expression Limit1 is valid when $\{-\phi_1 \leq \phi \leq \phi_1 \text{ and } \phi_2 \leq \phi \leq -\phi_2\}$ and Limit2 is valid when $\{\phi_1 \leq \phi \leq \phi_2 \text{ and } -\phi_2 \leq \phi \leq -\phi_1\}$

Similarly marginal PDF of the AoA in the elevation plane is found by integrating equation 3.16 with respect to azimuth angle ϕ with appropriate limits. The close form expression after tedious simplification for marginal PDF of AoA at MS are given below

$$P(\theta_{ms}) = \begin{cases} \frac{R^3 \phi_{ms} \cos[\theta_{ms}]}{2 \pi (R^3 - 2 (R - D \sin[\alpha])^2 (R + D \sin[\alpha]))} & ; \text{Limit 1} \\ \frac{D^3 \cos[\theta_{ms}] \sin[\alpha]^3 (1 - \sin[\theta_{ms}])^{3/2} (9 \sin[\phi_{ms}] + \sin[3 \phi_{ms}])}{24 \pi (R^3 - 2 (R - D \sin[\alpha])^2 (R + D \sin[\alpha]))} & ; \text{Limit 2} \end{cases} \quad (3.21)$$

In the above expression Limit1 is represents $\{\theta_{thresh} \leq \theta_{ms} \leq \pi/2\}$ and Limit2 is represent $\{0 \leq \theta_{ms} \leq \theta_{thresh}\}$.

Results and Discussions

In this chapter the results for different equation derived in chapter3 for the proposed 3D Hemisphere Model with Directional Antenna at BS are presented.

4.1 Threshold Elevation Angle θ_{thresh} as function of Azimuth Angle:

The threshold angle θ_{thresh} given by equation 3.9 is plotted in Figure 4.1 as a function of azimuth angles from 0 to 2π , for the beamwidth of the directional antenna $\alpha = 3^\circ$.

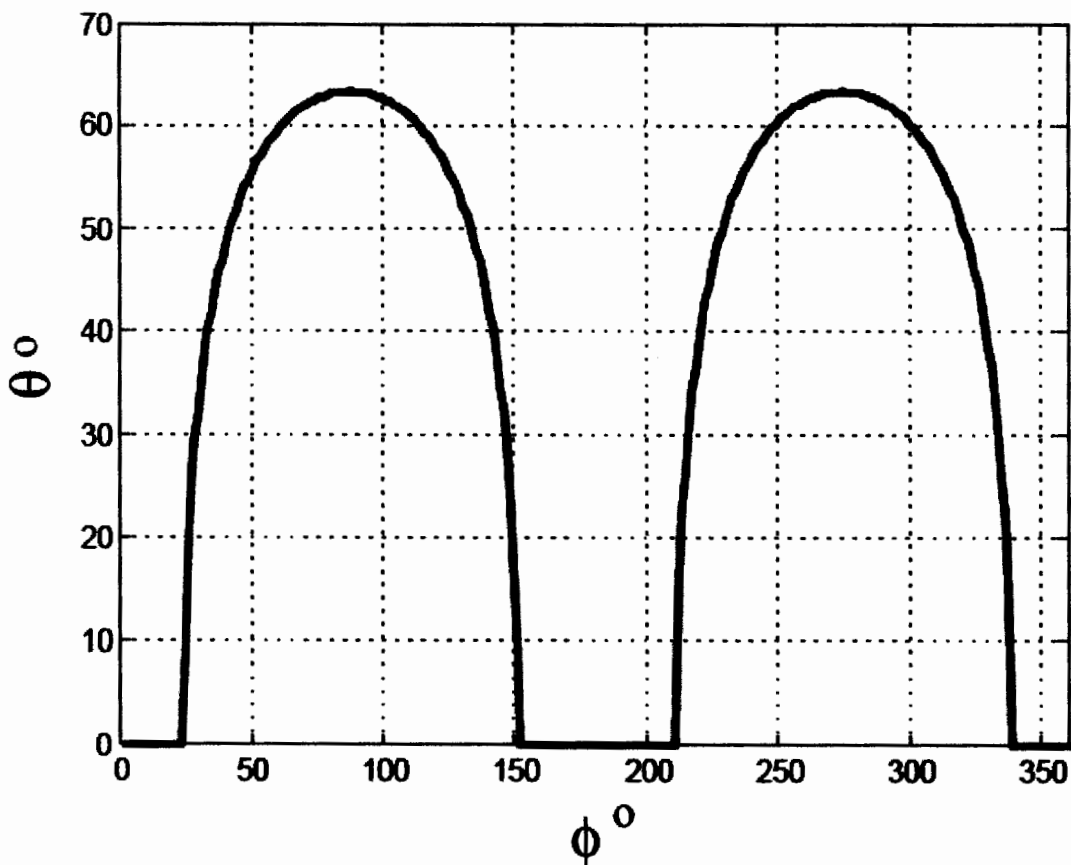


Figure4. 1: Threshold Angle θ_{thresh} in Azimuth Plane

4.2 Threshold Azimuth Angle “ Φ_{thresh} ” as function of Elevation Angle:

The threshold angle Φ_{thresh} given by equation 3.7 and 3.8 is plotted in Figure 4.2 as a function of elevation angles from 0 to $\pi/2$, for the beamwidth of the directional antenna $\alpha = 4^\circ$. Other parameter for this plot are, distance between the MS and BS, $D = 800\text{meters}$, Radius of the hemisphere $R = 100\text{meters}$

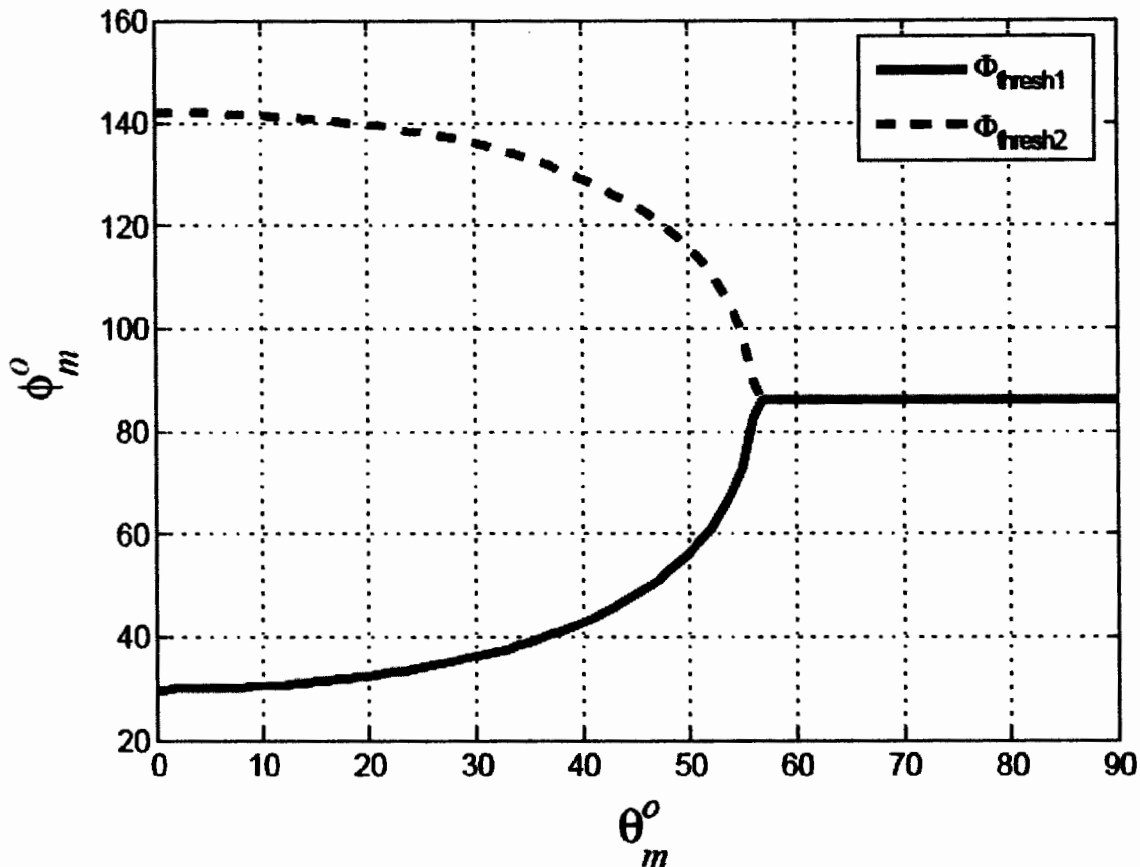


Figure4. 2: Threshold Angle Φ_{thresh} in elevation plane

4.3 Plot of length L “Distance between the MS and Scatterers”

Figure 4.3 shows the plot of length L in both azimuth and elevation plane derived in equation 3.12. From this plot the effect of directional antenna used at the BS can be observed. From the plot it is seen that for any particular azimuth angle ϕ there is a threshold angle θ_{thresh} in elevation plane. For $\theta > \theta_{\text{thresh}}$, the length L plotted here is seems to be uniform or constant, and

equals to the radius of the hemisphere which is taken 70m for this plot. In that case when it seems to be uniform, it follows the case of Omni directional antenna as shown in [11].

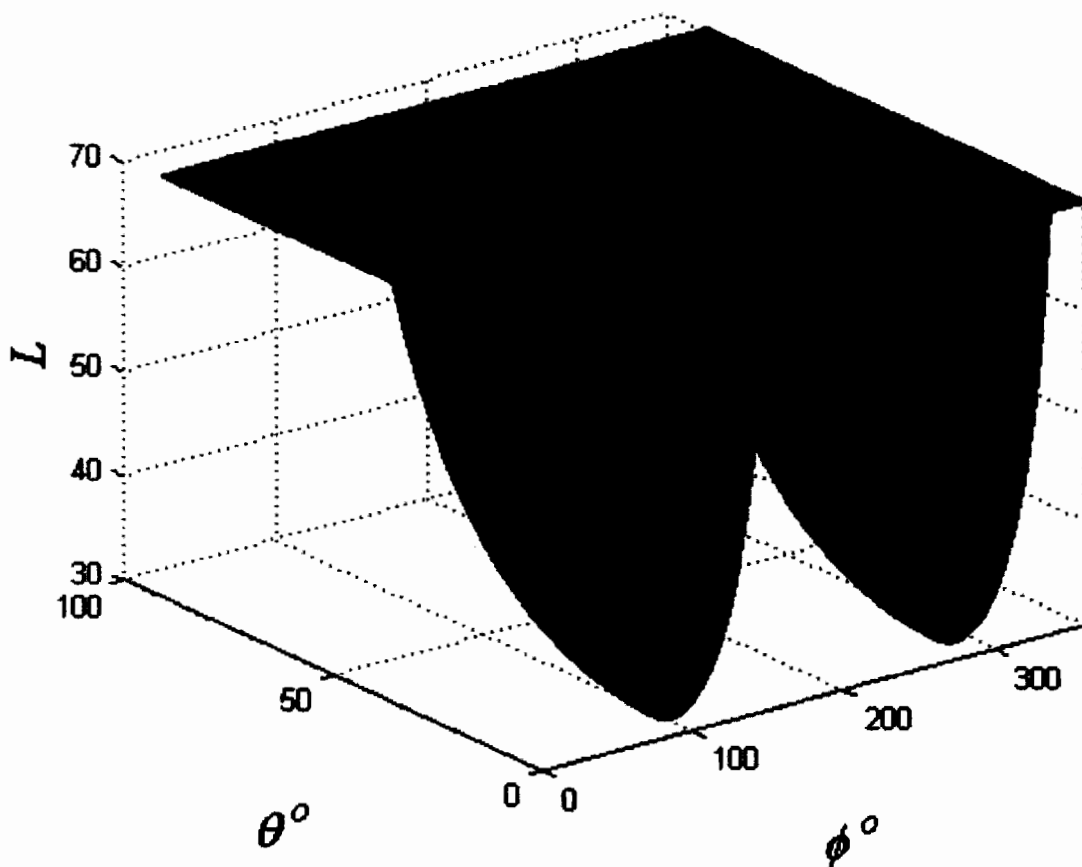


Figure4. 3: Length L as a Joint Function of Azimuth and Elevation Plane

The distance between the MS and the boundary of the hemisphere is same for $\theta > \theta_{\text{thresh}}$ in the azimuth plane, this means that all the scatterers would be illuminated. To elaborate this effect of directional antenna the same distance L derived in equation3.12 is plotted in Figure 4.4 in elevation plane for different azimuth angles i.e $\phi=0^\circ, 27^\circ, 35^\circ$ and 55° .

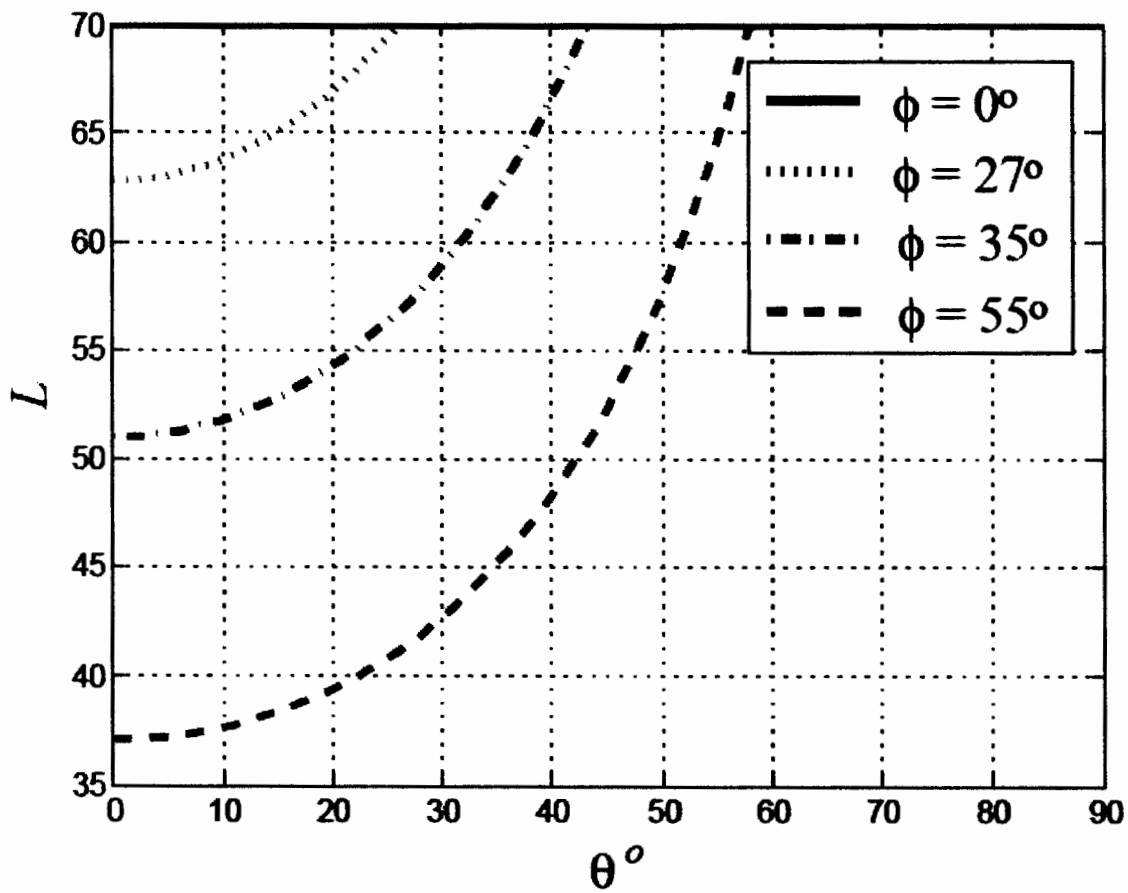


Figure 4. 4: Distance L In Elevation Plane.

It is clear from the above plot that when the azimuth angle $\Phi=0^\circ$, then the L is constant. Similarly L is plotted in azimuth plane for different elevation angle i.e $\theta=0^\circ, 30^\circ, 45^\circ$ and 55° , in Figure 4.5

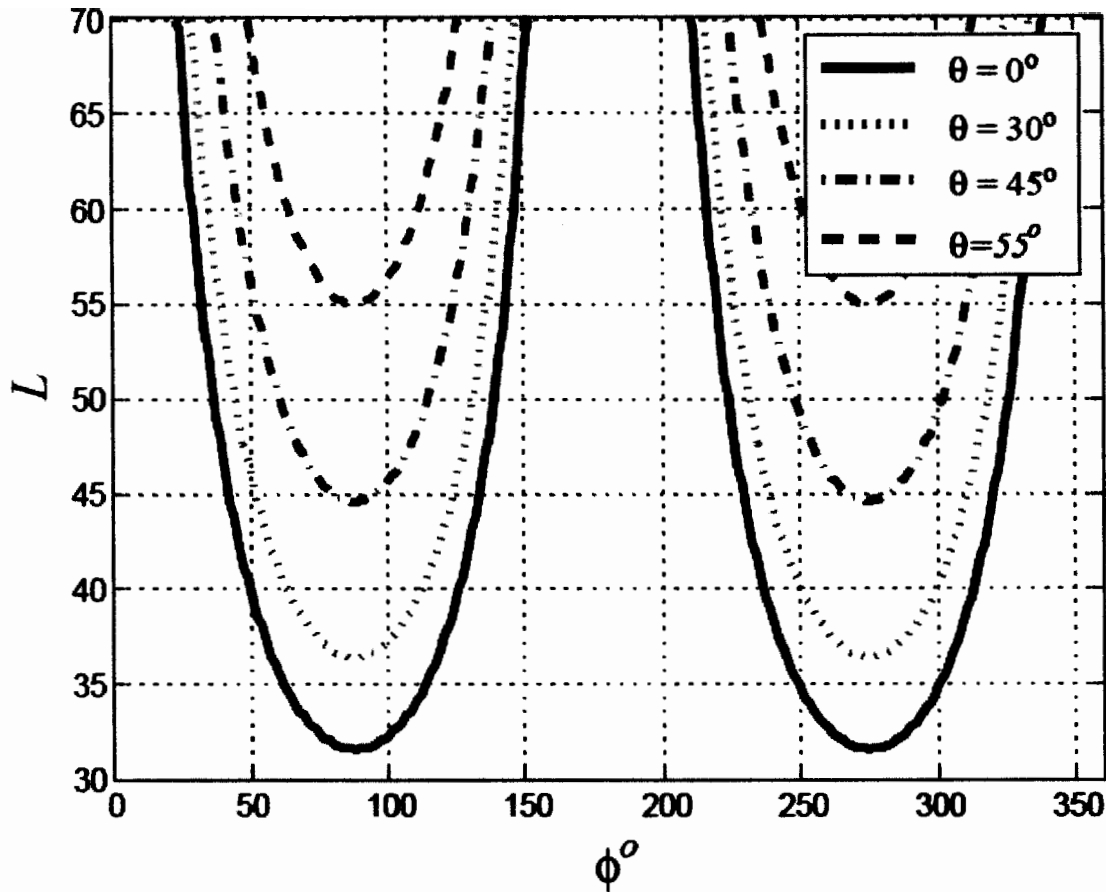


Figure4. 5: Distance L in Azimuth Plane for Different Elevation Angles

4.4 Analytical Results of PDF of AoA at MS.

In this section, the PDF of AoA derived in chapter 3 are plotted. The joint PDF of AoA at MS is given by equation 3.16 and plotted in Figure 4.6. The parameters for the proposed 3D hemisphere model with antenna array at the BS for all the plots presented in this section are as follow;

The distance D between the MS and BS = 600m, Radius R of the Proposed Model= 70m, the beamwidth of the direction antenna used at BS = 3° , Height Ht of the BS= 60m

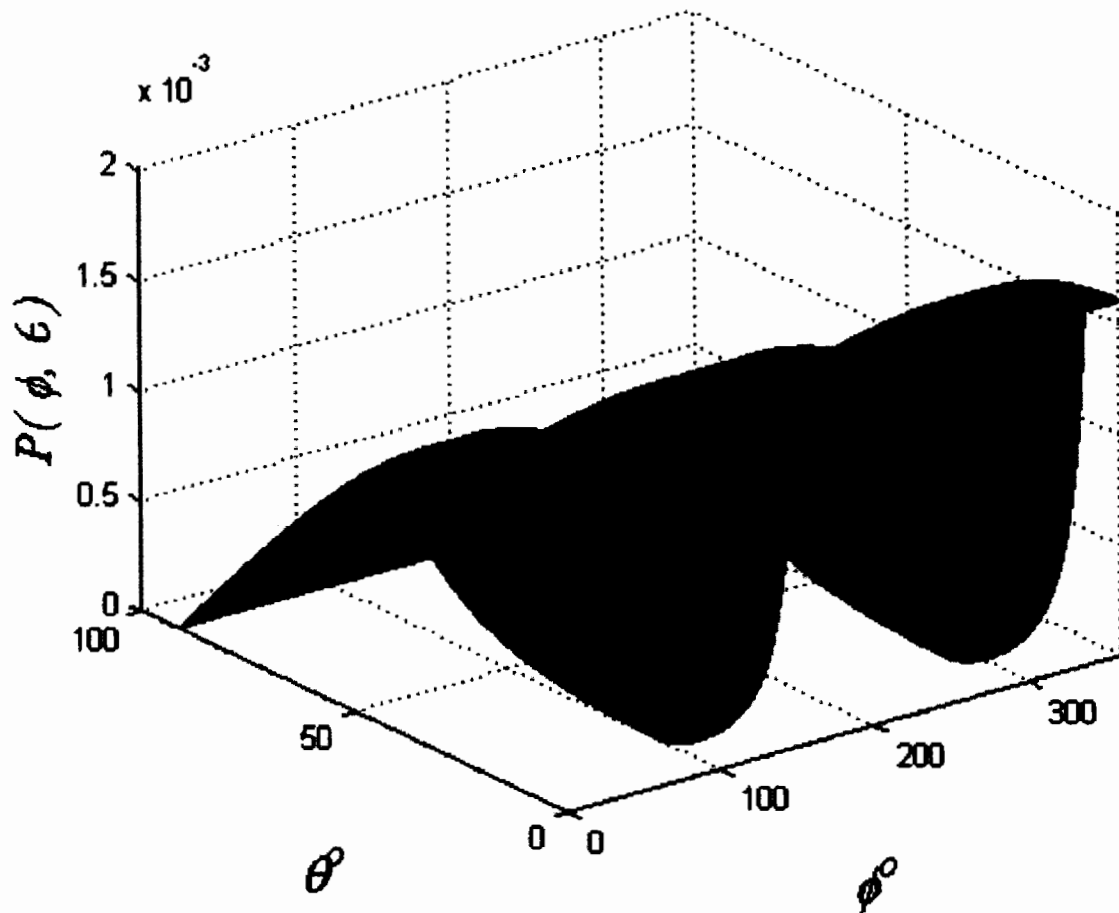


Figure4. 6: Joint PDF of AoA at MS for proposed 3D model

The AoA statistics at the MS with 3D uniformly distributed scattering region around the MS shown in the above figure as function of azimuth and elevation angles. The effect of directional antenna employed at the BS can also be analyzed with and help of this plot. The directional antenna used at the BS can adjust its beam pateren according to the AoA distribution and hence the same frequency can be used for multiple users at the same time interval (SDMA). And hence the capacity of the system will improve. Similarly the delay spread of the multipath components will decrease with its ability to adjust its beamwidth in a particular area of interest and avoid scatterers located away from the MS.

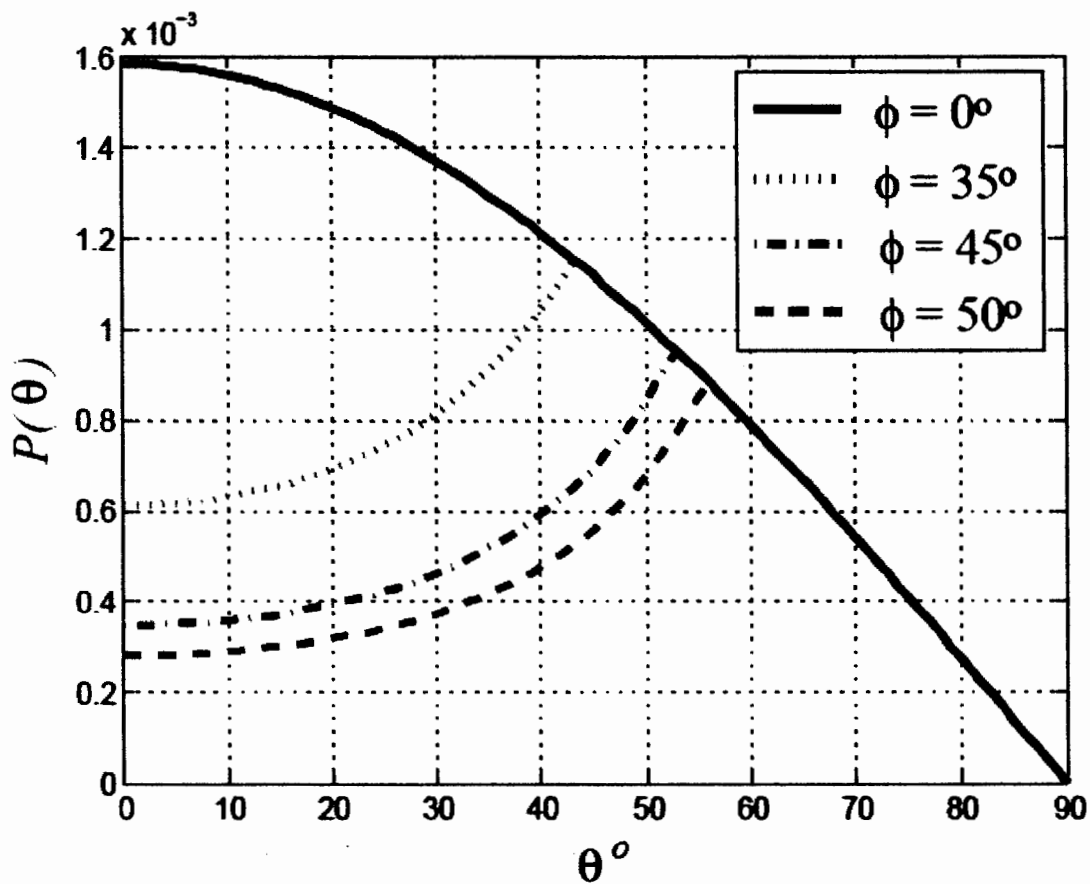


Figure 4. 7: Marginal PDF of AoA in Elevation Plane

Accurate knowledge of AoA statistics will help adaptive antenna array to avoid interference. And hence the quality of service will improve. In the proposed model used adaptive antenna array at the BS and also the scatterers are assumed to be uniformly distributed in a 3D hemisphere geometrical region, so the AoA statistics derived here are more precise as compare to 2D model. So taking the advantage of both directional antenna and 3D scattering, the proposed model will improve the quality of service by reducing interference and the capacity of the wireless system will enhance by using SDMA technique efficiently with the precise knowledge of the AoA statistics.

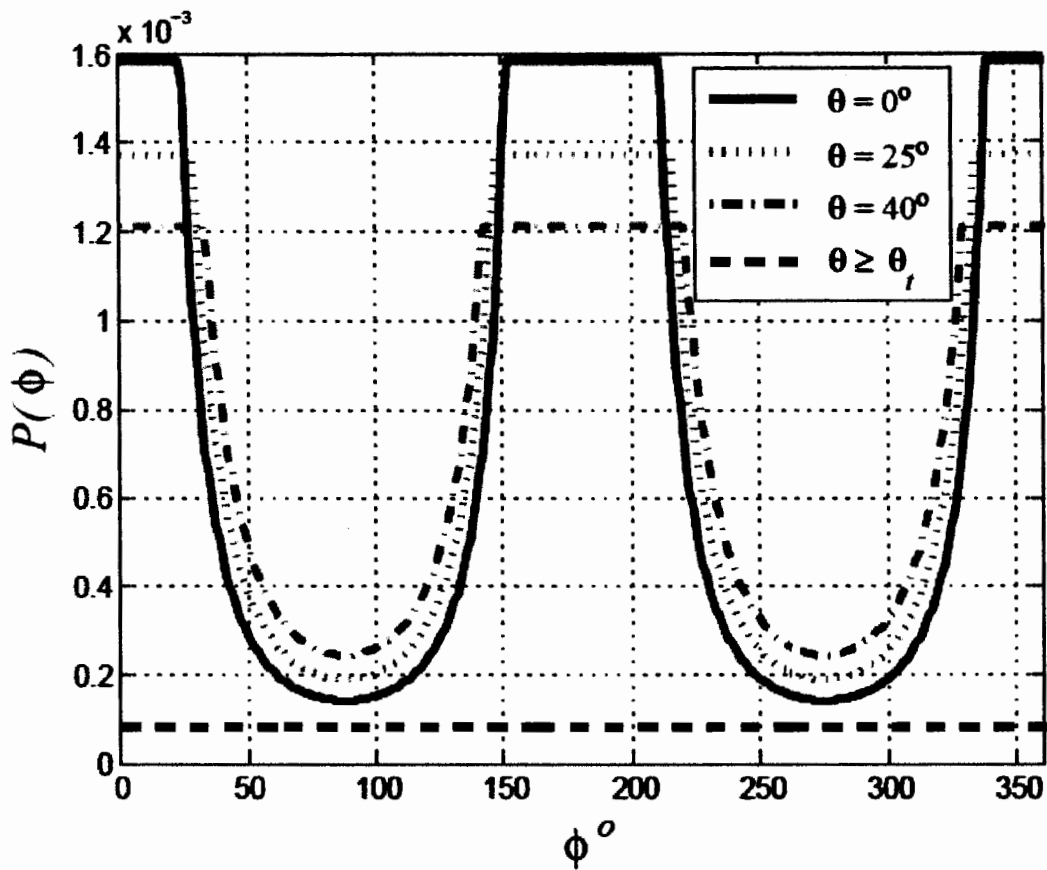


Figure4. 8: Marginal PDF of AoA In Azimuth Plane

Closed form expression 3.18 derived for the PDF of AoA in section 3.3, is plotted in Figure4.7 for different azimuth angles. Figure4.7 shows the marginal PDF of AoA in elevation plane for $\Phi=0^\circ, 35^\circ, 45^\circ$ and 50° . Similarly the Marginal PDF of AoA in azimuth plane is plotted for expression 3.17 derived in section3.3 for different ($\theta=0^\circ, 25^\circ, 40^\circ$ and $\theta \geq \theta_{\text{thresh}}$) elevation angles. Figure 4.8 shows that when $\theta \geq \theta_{\text{thresh}}$ this mean that the beamwidth “ α ” of the directional antenna is greater than or equal to the maximum beamwidth “ α_{max} ” as in case of omnidirectiona antenna used in [11]. Hence the effect of directional antenna for different elevation angles can be analyzed in Figure4.8 in azimuth plan for the proposed model.

4.5 Comparison with some notable models found in Literature

The results for marginal PDF of AoA obtained for the proposed model plotted in section4.4 deduces the results of Janaswamy Model proposed in [11] and GBSBM Petrus Model proposed in [11]. In 3D Spheroid Model proposed in [11] the MS is assumed to be located at the center of

semi-spheroid with uniformly distributed scatterers, whereas the BS is located outside the semi-spheroid in a scattering free region with omni-directional antenna as shown in Figure 2.11. The PDF of AoA in elevation plane for Janaswamy model is plotted in Figure 4.9.

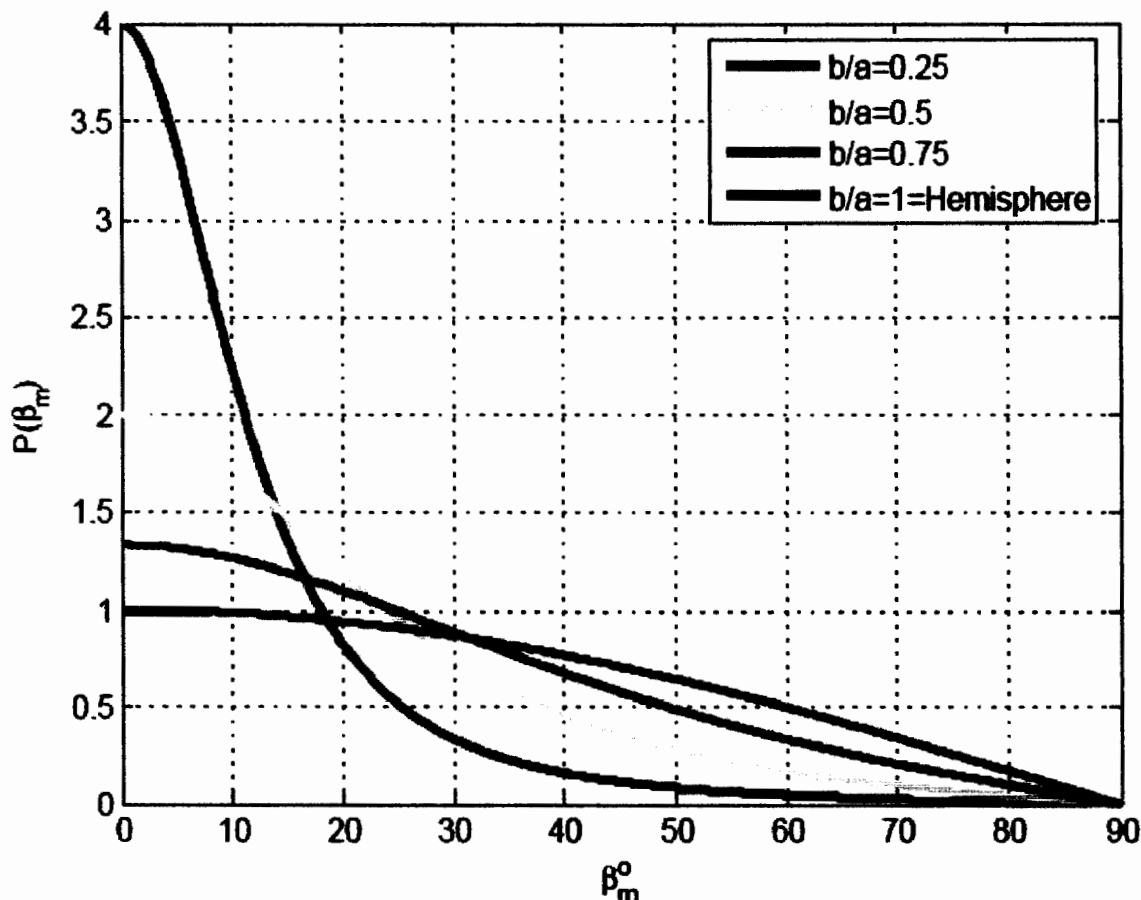


Figure4. 9: Marginal PDF of AoA in Elevation Plane for Janaswamy Model [11]

Note that when length of 'a' is equals to the length of 'b' for Spheroid in [11], the resultant geometry is equal the hemisphere of the proposed model. So the statistical result for AoA shown for this particular case (Figure 4.9 with red line) can be compared with the results of the proposed 3D Hemisphere Model. This comparison is shown by Figure 4.10.

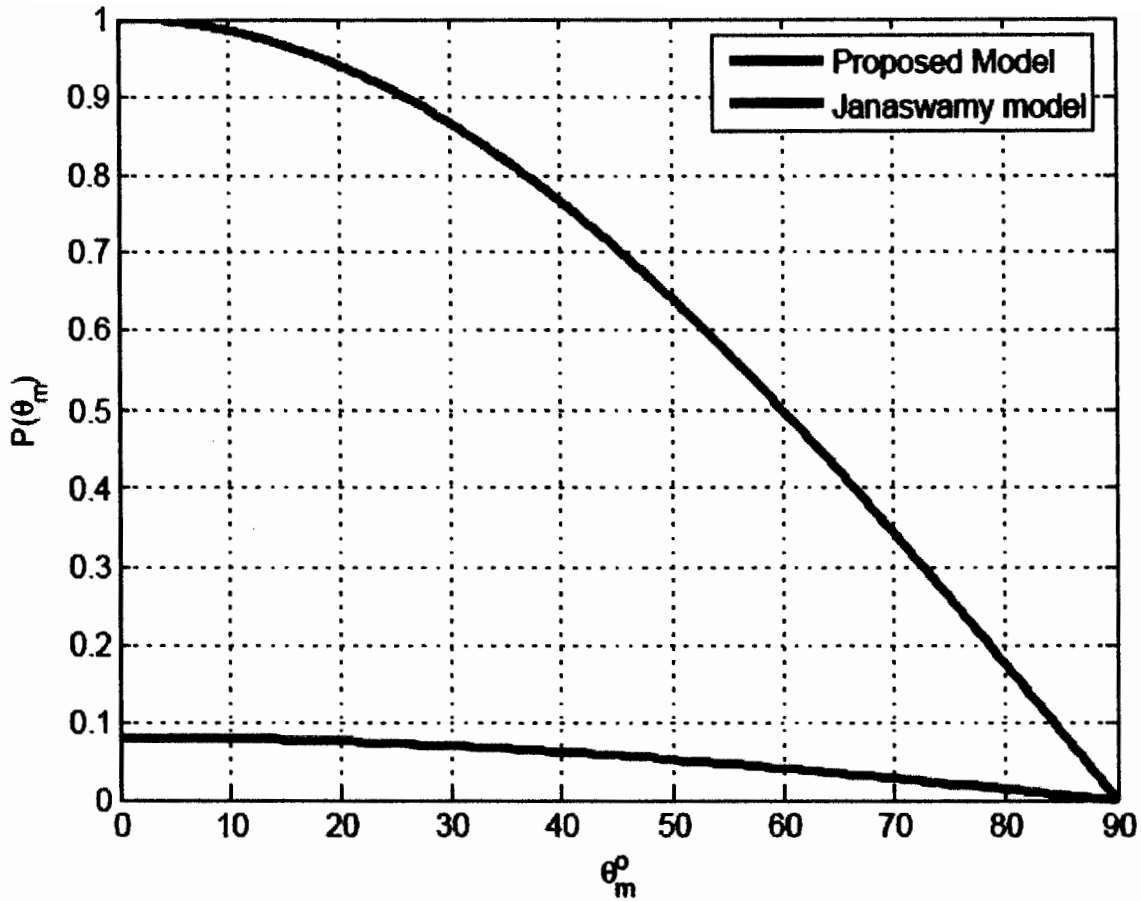


Figure4. 10: Comparison with Janaswamy Model [11]

It is clear from this comparison that probability of multipath components arriving from different angles are much lower than that of Janaswamy Model. This shows the effect of adaptive antenna array used at the BS for the proposed model. So with the use of smart antenna some of the multipath components can be avoid and hence less will be the interference so increased the quality of service.

Similarly the results of the PDF of the AoA in azimuth plane obtained for the proposed 3D hemisphere model deduces the results of 2D GBSBM proposed by Paul Petrus in [6]. The geometry of the GBSBM is shown in Figure 2.4. If we put elevation angle $\theta_{ms} = 0^\circ$, the propped 3D model reduces to 2D circular model, and hence it is almost equal to Petrus model. The PDF of AoA in azimuth plane plotted along with that of Petrus model in Figure 4.11. This plot shows that the proposed model verify the results of Petrus model.

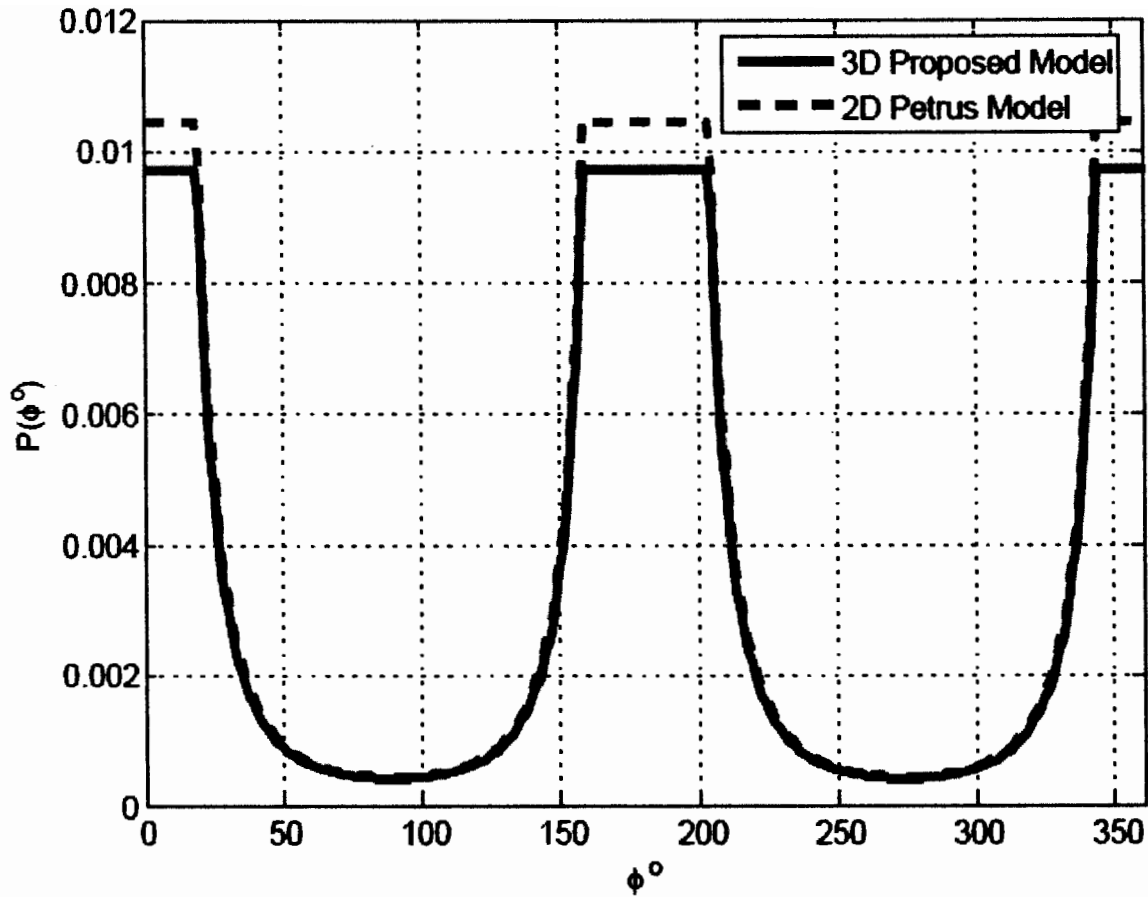


Figure4. 11: Comparison with 2D Petrus Model [6]

4.6 Effect of Adaptive Antenna Array on AoA Statistics

The effect of adaptive antenna array used at the BS for the proposed 3D Hemisphere Model can be analyzed by the plot shown in Figure 4.12. If we assume the beamwidth α equals to α_{max} , all of scatterers inside hemisphere gets illuminated. In such case the directional antenna used at the BS act as a omni-directional antenna. And hence the probability of multipath components arrived at the MS increases. Similarly if we assume beamwith $\alpha=3\alpha_0$, some of the scatterers of volume V_1 gets eliminated as illustrated in section 3.2, and hence the probability of multipath components arrives at the MS decreases. This scenario is shown in Figure 4.12. So with the use of adaptive antenna array at the BS quality of service will improve because of the mitigation of multipath components.

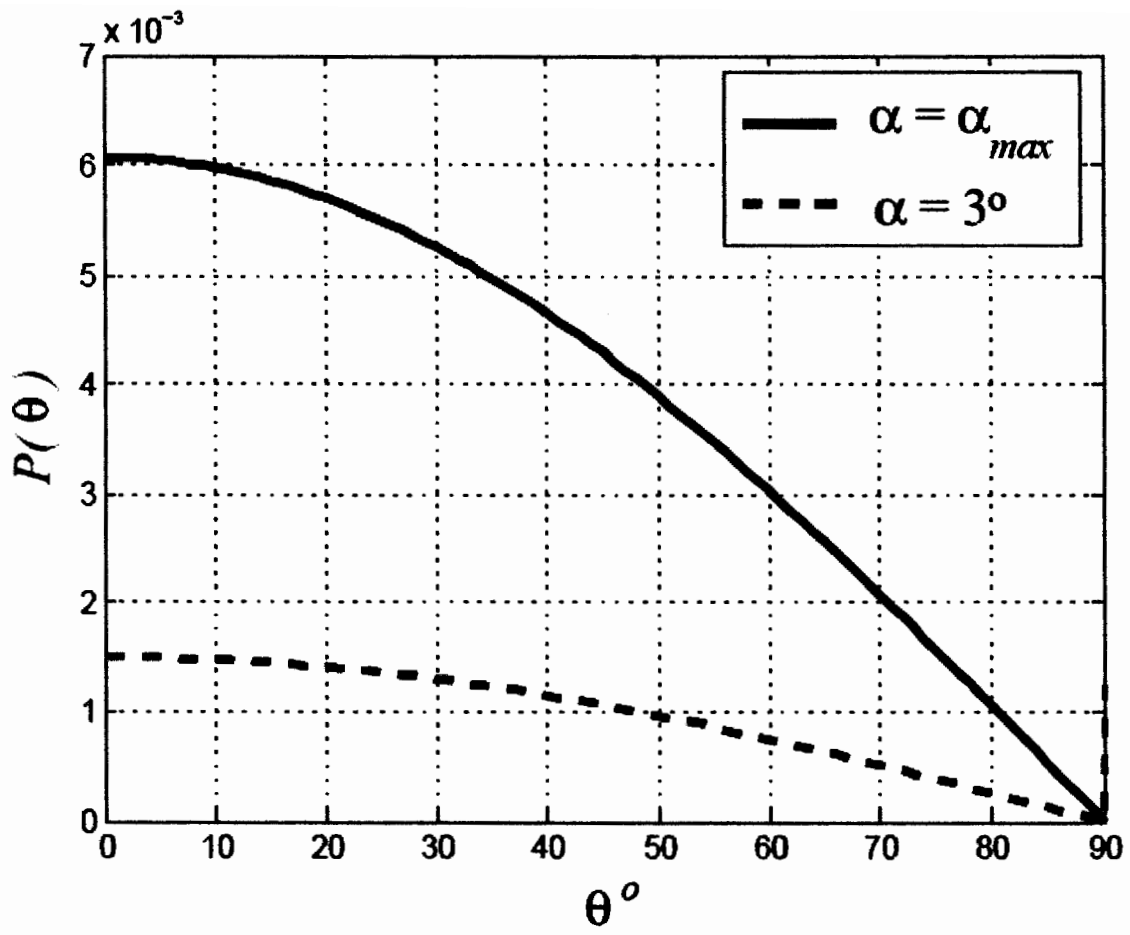


Figure4. 12: Effect of Adaptive Antenna Array of AoA Statistics

Conclusions and Future Research Plans

The summary of the work carried out for the thesis is presented in this chapter with some future research plans base on the results of the proposed model.

5.1 Summary of the Thesis

In this thesis we proposed a 3-D Hemisphere Model with Antenna Array at BS for the wireless radio environment and AoA statistics at MS are analyzed. It is assumed that the scatterers are uniformly distributed around the MS in the volume defined by the geometry of the hemisphere. It is also assumed that the MS is located at the center of the hemisphere and the BS is elevated at a height H_t with a Distance D from the MS. Joint and Marginal AoA statistics at the MS are mathematically derived in both azimuth and elevation planes. The main focus of the research was to investigate the effect of directional antenna on the spatial characteristics of the wireless radio channel in the presence of three dimensional scattering

In **Chapter No.1**, an overview of the wireless systems is presented with the history of capacity demand in wireless communication. It is described that how smart antenna technology can be used for capacity enhancement of the system. The importance of channel modeling is described with an introduction to AoA estimation. The overview of geometrical channel model is described with 2D and 3D geometrical channel models proposed in literature. The issues of the physical channel were discussed and the problem was formulated with the proposed methodology.

In **chapter No.2**, literature study has presented. 2D and 3D geometrical channel model proposed in recent literature were discussed.

In **Chapter No.3**, the proposed model is presented. The wireless radio environment is modeled with the assumption that the scatterers surround the MS in 3D hemisphere geometry. For the issue of capacity enhancement and quality of service the model is proposed with adaptive antenna array at the BS. The effect of directional antenna on the 3D is illustrated with some mathematical derivations. The volume of the scattering region is calculated and used for the

mathematical derivation of the PDF of AoA. Close form expression derived for the AoA statistics simultaneously in azimuth and elevation planes. Similarly close form expression are derived for marginal PDF of AoA at the MS.

In **Chapter No.4**, the results based on the mathematical derivation in chapter 3 are presented and discussed. In Figure 4.1 one the elevation threshold angle is plotted with respect to azimuth plane. In figure 4.2 the distance between the MS and the scatterer is plotted as a joint function of azimuth and elevation plane. Similarly the same function is plotted in azimuth and elevation plane in Figure 4.3 and 4.4 respectively. The PDF of AoA is plotted in Figure 4.5 as a joint function of azimuth and elevation angles. In Figure 4.6 the PDF of AoA is plotted in elevation plane and in Figure 4.7 the PDF of AoA is plotted in azimuth plane. The effect of directional antenna is discussed with the analysis of all the result in the same chapter.

It is concluded that with the use of directional antenna used at the BS for the proposed model, and the precise knowledge of the AoA, will enhance the system capacity and will improve the quality of service.

5.2 Future research plans

The future research planes are as follow

5.2.1 Research Plan 1

In the proposed 3D hemisphere model with directional antenna at the BS the beamwidth is controlled in azimuth plane. The spatial characteristics of the wireless channel have never been investigated where the beamwidth is controlled in elevation plane.

5.2.2 Research Plan 2

The PDF of the AoA derived [11] are used in [19] to analyze the Doppler Shift distribution of the received signal in 3D wireless environment. Similarly results of the present thesis particularly by section 3.3 can be used to analyze the effect of directional antenna of Doppler shift as done by Shouxing in [19].

References:

- [1] A. J. Paulraj, D. A. Gore, R. U. Nabar and H. Bölcskei "An overview of MIMO communications: A key to Gigabit wireless," Proc. IEEE, vol. 92, no. 2, pp. 198-218, February 2004.
- [2] N. M. Khan, M. T. Simsim and P. B. Rapajic "A Generalized model for the spatial characteristics of cellular mobile channel," IEEE Trans. Veh. Technol., vol. 57, no. 1, January 2008.
- [3] JACK H. WINTERS "Smart Antennas for Wireless Svsvfems" IEEEd Personal Communications February 1998
- [4] Frank B. Grass "Smart Antenna for Wireless Communication with Matlab"
- [5] T.S Rappaport "Wireless Communication Prinicipal & Practice"
- [6] P. Petrus, J. H. Reed and T. S. Rappaport "Geometrical-based statistical macrocell channel model for mobile environments," IEEE Trans. Commun., vol. 50, no. 3, pp. 495-502, March 2002.
- [7] R. B Ertel and J. H Reed "Angle and time of arrival statistics for circular and elliptical scattering models," IEEE J. Sel. Areas Commun., vol. 17, no. 11, pp. 1829-1840, November 1999.
- [8] J. C. Liberti and T. S. Rappaport, "A Geometrically Based Model for Line-of-Sight Multipath Radio Channels," Proc. of IEEE Veh. Tech. Conf. pp. 844-848., Apr. 1996.
- [9] R. Janaswamy "Angle and time of arrival statistics for the Gaussian scatter density model," IEEE Trans. Wireless Commun., vol. 1, no. 3, pp. 488-497, July 2002.
- [10] M. P. Lotter and P. V. Rooyen "Modeling Spatial Aspects of Cellular CDMA / SDMA Systems," IEEE Commun. Lett., vol. 3, no. 5, pp.128-131, May 1999.
- [11] R. Janaswamy "Angle of arrival statistics for a 3-D Spheroid Model," IEEE Trnas, veh. technol., vol. 51, no.5, pp. 1242-1247, September 2002.

- [12] K. B. Baltics and J. N. Saholas "A simple 3-D geometric channel model for macrocell mobile communication," Springer Wireless Personal Communication, DOI 10.1007/s 11277-008-9464-3, November 2008.
- [13] I. Jaafar, H. Boujem and M.Siala "Angle and time of arrival statistics for hollow-disc and elliptical scattering models" 2nd Int. Signal, Circuit and Systems (CCS)., pp-1-4, Nov. 2008.
- [14] Sami A. Mostafa, S. H. Elramly, and Meriam K. Ragheb "Adaptation of Angle-of Arrival Estimation in Mobile Communications Using Geometrically Based Channel Models"
- [15] A. Y. Olenko, k. T. Wong, S. A. Qasmi and J. A. Shokouh "Analytically derived Uplink/downlink ToA and 2-D DoA distributions with scatterers in a 3-D hemispheroid surrounding the mobile," IEEE Trnas, Antennas and Propagation., vol. 54, no.9, pp. 2446-2454, September 2006.
- [16] S. Qu and T. Yeap "A three dimensional scattering model for fading channels in land mobile environment," IEEE Trnas, veh. technol., vol. 48, no.5, pp. 765-781, May 1999.
- [17] G.D. Durgin, T.S. Rappaport. "Theory of Multipath Shape Factors for Small-Scale Fading Wireless Channels," IEEE Transactions on Antennas and Propagation, vol. 28, no-5, pp. 682-693, April 2000.
- [18] Richard B. Ertel, Paulo Cardieri, Theodore S. Rappaport and Jeffrey H. Reed, "Overview of Spatial Channel Models for Antenna Array Communication Systems" IEEE Personal communication, pp10-22, feb1998
- [19] shouxing qu. "An analysis of PDF of Doppler Shift in three Dimensional mobile radio environment". IEEE Trans Veh tech may 2009.
- [20] Noor. M. Khan "Modeling and Characterization of Multipath Fading Channels in Cellular Mobile Communication Systems ," *PhD Thesis UNSW*, Australia , 2006.
- [21] Khoa N. Le "On Angle-of-Arrival and Time-of-Arrival Statistics of Geometric Scattering Channels" IEEE TRANSACTIONS ON VEHICULAR TECHNOLOGY, VOL. 58, NO. 8, OCTOBER 2009

